Universidade de Aveiro Departamento de Engenharia de Materiais e Cerâmica
2014

Neda Eghtesadi

Mechanical properties of resorbable PCL/FastOs®BG composite materials

Universidade de Aveiro Departamento de Engenharia de Materiais e Cerâmica
2014

Neda Eghtesadi

Mechanical properties of resorbable PCL/FastOs®BG composite materials

Dissertation submitted to the University of Aveiro to fulfill the requirements for obtaining a Master's degree in Materials and Biomedical Devices. This work was performed under the scientific guidance of Prof. José Maria da Fonte Ferreira, Department of Materials Engineering and Ceramic of University of Aveiro

This thesis is dedicated to my parents for their love, endless support and encouragement.

o júri

Presidente

Prof. António Manuel Godinho Completo
Professor Auxiliar, departamento de Eng.ª Mecânica, Universidade de Aveiro

Arguente:

Prof. José Martinho Marques de Oliveira
Director da Escola Superior de Design, Gestão e Tecnologias da Produção Aveiro Norte
Universidade de Aveiro

Supervisor

Prof. José Maria da Fonte Ferreira
Professor Associado c/ Agregação, departamento de Engenharia de Materiais e Cerâmica, Universidade de Aveiro

Acknowledgment

It is an honour for me to express gratitude and thank to my advisor, Prof. José Maria da Fonte Ferreira, for his leading role and great support during the entire time of my studies, as well as personal support he always provided. I would like to thank the entire staff of the Mechanical Department of University of Aveiro, particularly Prof. António Completo, Prof. António Bastos, Ricardo N. Beja and Saied Tamimi for providing such a good and friendly working environment, lab space and also technical support. I owe my deep gratitude to Sandra Pereira Magina, Ana Isabel da Graça Barranqueiro Caço and Carla Vilela from CICECO for discussions and support of my work. My thanks and appreciation to Avito Rebelo for his friendship and strong support regarding to his expertness and great taste in programming and designing.

Thanks to my friends, who have been supporting me during difficult times. I will not forget. I will be always ready to give it back. As well I will never forget all strong good and clever people I have met. Thank you just for being and giving me the strength to believe that the right way is still not empty.
The last but the most I want to thank my family, especially my parents who faced out the hard times with me. They gave me the absolute freedom in my decisions and maximal possible support.

Palavras-chave Policaprolactona, Biovidro, Materiais compósitos, Propiedades mecânicas, Ortopedia.

Resumo

Compósitos biorreabsorvíveis desempenham hoje em dia um papel cada vez mais importante na medicina moderna, especialmente em ortopedia para a fixação de fracturas ósseas e de tendões. Contrariamente aos dispositivos metálicos, eles evitam uma segunda intervenção cirúrgica para os remover, sendo gradualmente integrados nos tecidos ósseos. Encontrar maneiras de melhorar suas propriedades físicas e mecânicas para melhor atender as condições e ambientes específicos a que se destinam tem sido uma meta estabelecida em vários trabalhos de investigação. Com base nesses trabalhos, foi possível estabelecer que o tamanho, a forma e a razão de aspecto, bem como a fracção volúmica das partículas de reforço constituem os principais parâmetros que afectam as propriedades mecânicas de um compósito. O objectivo deste trabalho é investigar o efeito da adição de diferentes proporções de partículas do vidro bioativo FastOs®BG Di–70 nas propriedades mecânicas de policaprolactona (PCL) usada como matriz. A selecção desta matriz foi baseada num conjunto de propriedades interessantes que possui, incluindo o facto de ter sido aprovada pela FDA para aplicações biomédicas e ser relativamente barata.

As principais desvantagens da PCL estão relacionados com a sua natureza relativamente hidrofóbica, e com uma taxa de degradação lenta *in vivo* (até 3-4 anos). O presente trabalho tem uma finalidade múltipla e visa a superação e / ou mitigar as principais limitações identificadas para a PCL, ou seja, melhorar as propriedades mecânicas relevantes, acelerar a taxa de biodegradação *in vivo*, e tornar os materiais compósitos bioactivos. Para o efeito seleccionou-se o biovidro FastOs®BG Di–70 na forma de pó como material de enchimento.

Este biovidro é caracterizado por uma elevada taxa de biomineralização *in vitro*, tem um caracter mais hidrófilo e um módulo de elasticidade mais elevado. Assim, da combinação em proporções diferentes de PCL-FastOs®BG Di–70, espera-se que resultem materiais compósitos com um conjunto mais equilibrado de propriedades para as aplicações almejadas. As propriedades mecânicas dos compósitos foram avaliadas sob diferentes modos de teste (de tração, compressão, torção e oscilatórios).

Keywords Polycaprolactone, Bioactive glass, Composites, Mechanical properties, Orthopaedics.

Abstract

Bioresorbable composites nowadays play an increasingly important role in the modern medicine, especially in orthopaedics for the fixation of bone fractures and tendons. Contrarily to the metallic counterparts, they prevent a second surgical operation to remove them, because they will be gradually integrated in the bone tissues. Finding ways to improve their physical and mechanical properties to better fit the intended specific conditions and environments has been a goal in many researches. It has already established that size, shape, aspect ratio and volume fraction of reinforcing particles are parameters which can effect on mechanical properties of a composite. The aim of this work is to investigate the effect of different proportion of particulate FastOs®BG Di–70 bioactive glass filler on the mechanical properties of polycaprolactone (PCL) matrix. The selection of the PCL was based on its set of interesting properties, including the FDA approval for biomedical applications and the relatively low cost.

The main drawbacks of PCL are related to its relatively hydrophobic nature and the slow degradation rate it undergoes *in vivo* (up to 3-4 years). The present work has a multifold purpose and aims at overcoming and/or mitigating the main identifies limitations of PCL, namely enhancing relevant mechanical properties, fastening the biodegradation rate in vivo, and turning the material bioactive. For this, FastOs®BG Di–70 bioglass powder was selected as filler.

This bioglass is characterised by a high biomineralisation rate in vitro, has a more hydrophilic character and higher Young modulus. The combination of PCL-FastOs®BG Di–70 bioglass in different proportions is therefore expected to confer to the composites a more balanced set of properties for the intended applications. The mechanical properties of composites were assessed under different testing modes (tensile, compressive, oscillatory and torsional).

Contents

.....

CHAPTER 1

1.1 Introduction

Despite bioresorbable polymers are increasingly being considered as good alternatives for metal implant devices due to intrinsic properties and they could solve a set of existing problems with metal implants, they still suffer from some limitations regarding to mechanical and bioresorbability properties. One of the most serious limitations of biodegradable implants is their lower mechanical strength in comparison to metal implants. Another major concern with bioresorbable polymers is related to their degradation time in the body. Since bioresorbable polymeric compounds and devices are designed with the aim of helping the body function for a limited period of time, i.e. the healing time, so the main goal in the case of internal fixation devices such as pins, screws, staples, etc., is that materials should retain adequate strength over time to be effective in fracture healing. But also these implants need to undergo hydrolysis over time and be eliminated after a certain time[1][2].

Polycaprolactone (PCL) was extensively investigated as a biomaterial during last two decades. Applying PCL as a bioresorbable polymer shows less stress shielding than metal devices. PCL shows superior rheological and viscoelastic properties over many of its aliphatic polyester counterparts. These properties make it easy to manufacture and manipulate into a large range of implants and devices. Despite its remarkable properties, using pure PCL in orthopaedic applications is very rare due to its poor mechanical strength for load bearing applications. Blending PCL with other materials can produce superior copolymers and composites which may have desirable properties like higher mechanical strength or higher bioactivity for use in applications where more resilient or higher bioactive materials are needed[1][3][4].

1.2. Study Motivation

From the materials science point of view, a single material type does not usually provide the necessary mechanical and/or chemical properties required. Hence, the properties of two or more materials can be smartly combined in a composite material that might exhibit key properties for an intended application [5][6].

In comparison to homogeneous materials, composites have plenty of advantages. Composites have the potential to produce hard, strong and light materials, with complex properties [7][8]. The properties of composites severely depend on a number factors including: (i) the volume fractions occupied by the component materials; (ii) the size and shape/morphology features of the embedded component; (iii) the interfacial bonding strength between different constituents; (iv) the presence/absence of microstructural heterogeneities; etc. The motivation behind the present research is to combine the attractive properties (mechanical, non-cytotoxicity) of polycaprolactone with the excellent bioactivity of a bioactive glass, FastOs®BG Di–70, to obtain a composite material with improved bioactivity and biodegradability in comparison to those of PCL alone, which could be suitable for applying in fixation of tendons and bone fractures.

The polymer matrix plays a critical role in providing the necessary mechanical stability to constructs. On the other hand, bioactive glasses have the ability to degrade *in vivo* and are ideal candidates for being incorporated in the composite with polymeric matrix to confer them the ability to be gradually degrade while offering an active surface for bone growth and the replacement of the implant materials [9][10]. Provided that the degradation rate of the implant materials and the rate of bone growth match, the required conditions for a strong bond with the living bone tissue are met [10][11].

1.3 Project aims

The aim of this work is to investigate the effect of adding different proportions of Diopside bioactive glass filler particles to a PCL matrix on the mechanical properties of composite materials. For this purpose, the relatively hydrophobic polycaprolactone polyester with a typically slow degradation rate (up to 3–4 years) was combined with the selected FastOs®BG Di–70 powder as filler as an attempt to enhance the hydrophilic character of the composites and foster their bioactivity and degradation rate. It

has been proved by several theories that mechanical properties of particulate reinforced polymer composites strongly depend on the particle size, particle–matrix interface adhesion and particle loading [9][12][13]. In the present work, the effects of different filler volume fractions on the mechanical properties and degradation rate of the composite will be investigated. It is expected that a better balance of these relevant properties will be obtained for the PCL/FastOs®BG Di–70 composites.

1.4 Outline of the thesis

I. Chapter one (Introduction) briefly introduces the theme of the thesis and explains the main aims of this work and the motivations behind it, namely a novel attempt for solving the problems related to the slow degradation rate and poor bioactivity of PCL by adding a bioactive glass powder with an excellent in vitro biomineralization activity, FastOs®BG-Di-70.

II. Chapter two describes the state of the art concerning the relevant factors involved in bone healing and the role of bioresorbable fixation systems for bone fractures and tendons. An historical account about the development process of fixation devices is presented in a brief literature review about related works carried out by others in the past.

III. Chapter three is about methodology. It describes how testing and validation tasks were performed. Plans and strategies used in this work, integration testing and system testing are described in this section. Test plans, procedures for testing and test tools are described in this chapter.

IV. Chapter four (Results and discussion chapter) presents the experimental results collected along this thesis and attempts to interpret them in a consistent manner in order to highlight their meaningfulness.

V. Chapter five (conclusions) gives a general overview about the main findings achieved in this thesis and points out the points that need further attention in future research works.

CHAPTER 2

2.1. Bone structure

The main role of the musculoskeletal system is to transmit forces from one part of the body to other organs. Several skeletal tissues participate in this mechanical objective of transmission and protection: bone, cartilage, tendons, ligaments and muscles. Bone mainly determines global structural stiffness and strength, whereas other tissues transmit loads between bones. Bone tissue has very interesting structural properties. This is essentially due to the composite structure of bone, composed by hydroxyapatite, collagen, and small amounts of proteoglycans, non-collagenous proteins and water. This composition varies with species, age, sex, the specific bone and whether or not the bone is affected by a disease [14][15].

From a macroscopic point of view, bone tissue is non-homogeneous, porous and anisotropic. Although porosity can vary continuously from 5 to 95%, most bone tissues have either very low or very high porosity. Accordingly, there is a distinction between the two types of bone tissues. The first type is trabecular or cancellous bone with 50–95% porosity, usually found in cuboidal bones, flat bones and at the ends of long bones. The pores are interconnected and filled with marrow whose main function is to produce the basic blood cells). The second type is cortical or compact bone with 5–10% porosity and different types of pores [16]. Cortical bone consists of cylindrical structures known as osteons or Haversian systems (Fig. 2.1).

Bones can grow, modify their shape (external remodelling or modelling), self-repair when fractured (fracture healing) and continuously renew themselves by internal remodelling. All these processes are governed by mechanical, hormonal and physiological patterns. Osteoblasts are the differentiated mesenchymal cells that produce bone. They are created at the periosteum layer or stromal tissue of bone marrow. Osteoclasts remove bone, demineralising it with acid and dissolving collagen with enzymes. These cells originate from the bone marrow. Bone lining cells are inactive osteoblasts that are not buried in new bone. They remain on the surface when bone formation stops and can be reactivated in response to chemical and/or mechanical stimuli [17]. Like bone lining cells,

osteocytes are former osteoblasts that are buried in the bone matrix. They are located in lacunae [16] and communicate with the rest of cells via canaliculi.

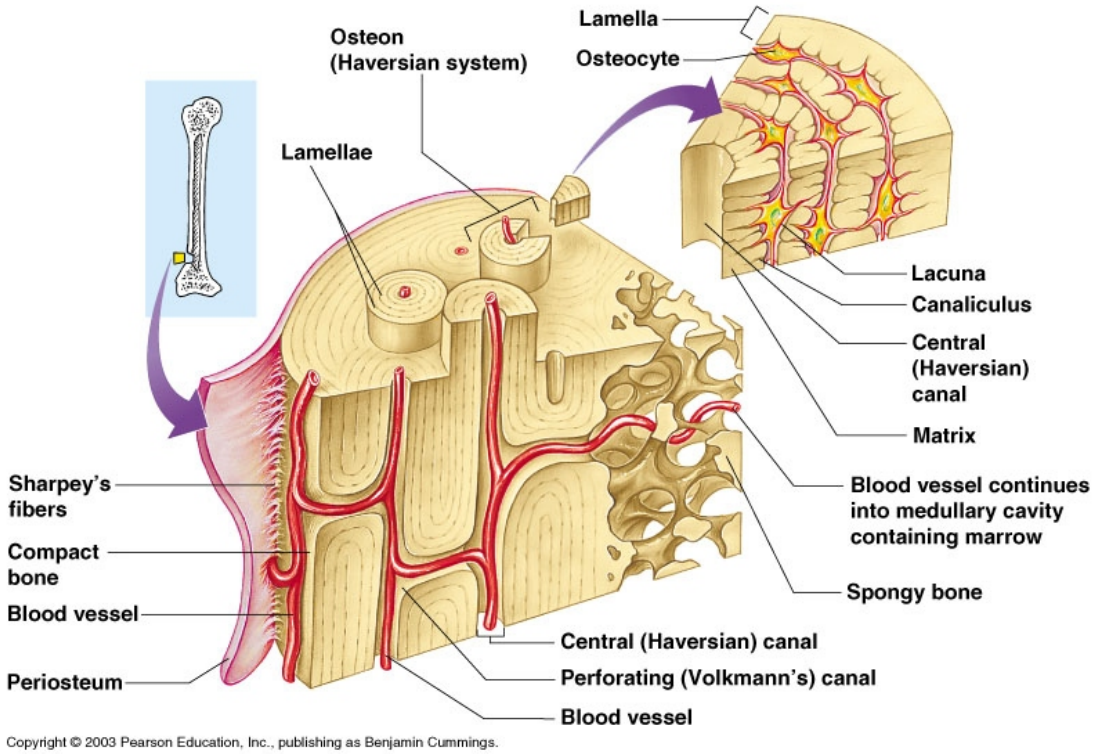

Figure 2.1: Microscopically structure of cortical bone - 3D sketch of cortical bone and cut of a Haversian system

2.2. Bone fractures and fracture healing process

The goals in the treatment bone fractures are restoring the functional abilities as soon as possible and preventing the occurrence of subsequent fractures. The structural grafts may be biologically inert or osteoinductive, and various osteoinductive growth factors and hormones may be needed to supplement the treatment. Several types of external fixation devices (screws, various plates, tension band wiring, threaded K-pins, etc.) have improved the clinical outcome in terms of osteosynthesis.

Fracture healing is a complex reparative process that involves inflammation, growth, tissue differentiation, ossification and remodelling. All these processes evolve at the same time in different regions of the fracture site, regulated by the mechanical conditions and the local vascularity. A precondition of healing is that by tissue differentiation and callus formation the fracture is stabilised enough to allow for bone formation. Later, when the callus is large enough, these cells may differentiate into chondrocytes, osteoblasts or fibroblasts, depending on the biological and mechanical conditions. Intramembranous woven bone formation appears adjacent to each side of the gap site, advancing to the centre of the callus. This type of ossification is produced by direct differentiation of the stem cells into osteoblasts, producing bone tissue. At the same time in the centre of the callus, cartilage is formed by chondrogenesis, except for the site very close to the gap, where the stability is still very small (Figure 2.2).

Once that the callus is filled mainly by cartilage, endochondral ossification begins coupling a complex sequence of cellular events: cartilage maturation and degradation, vascularity and osteogenesis. This ossification continues until all the cartilage has been replaced by bone and an entirely bony bridge closes the fracture gap achieving a good stabilization and sufficient stiffness. Once the gap has ossified, remodelling of the fracture site begins gradually in order to restore its original form and internal structure of the bone, which takes longer time in comparison to previous steps [18][19].

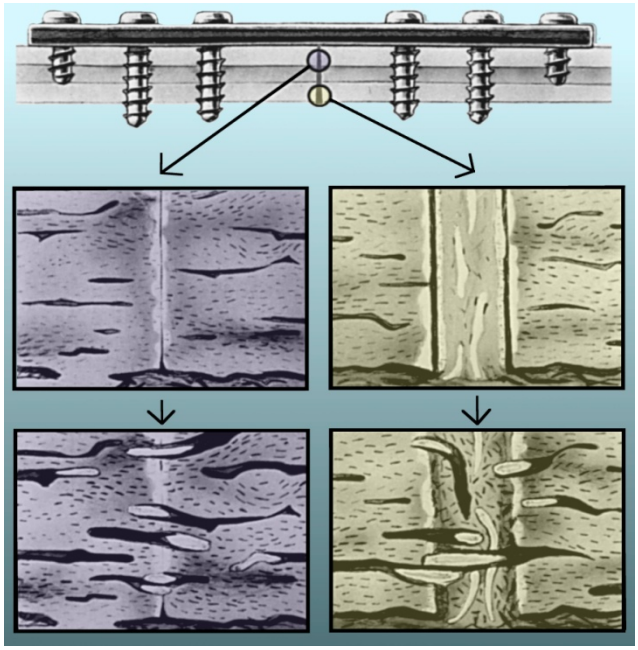

Figure 2.2: Fracture healing patterns [20]

2.3. Implants and fixation devices

Rigid fixation of long bone fractures is often achieve surgically using metal plates and screws to align and hold the bone fragments. The performance of implants comprises two components, the response of the host to the implant and the behaviour of the material in the host [21]. Therefore, they have to meet mechanical and biological requirements to fulfil the categorisation of the objectives specified in its design. They have to respond to the demands of providing mechanical support, inducing or conducting bone formation and an easy removing when their function is no longer needed.

Implants are always in contact with living tissue, so interface reactions always occur on the macro-micro- and/or nanoscale and may be initiated by biological, chemical, thermal or physical reactions. Therefore, the main property to be considered in the design of implants and prostheses is biocompatibility, which is defined as: “The ability of a material to perform with an appropriate host response in a specific application”. This definition includes two aspects: the biological and the functional compatibility. Figure 2.3 shows different composite biomaterials applications in body.

Properties such as biological safety, corrosion resistance, degradation, elasticity, ductility, strength and fatigue behaviour depend mainly on the materials that compose the implant, as well as the way they are processed. However, the geometrical design, the surface treatment, the fracture type and the surgical technique are also essential in evaluating the performance of a specific device.

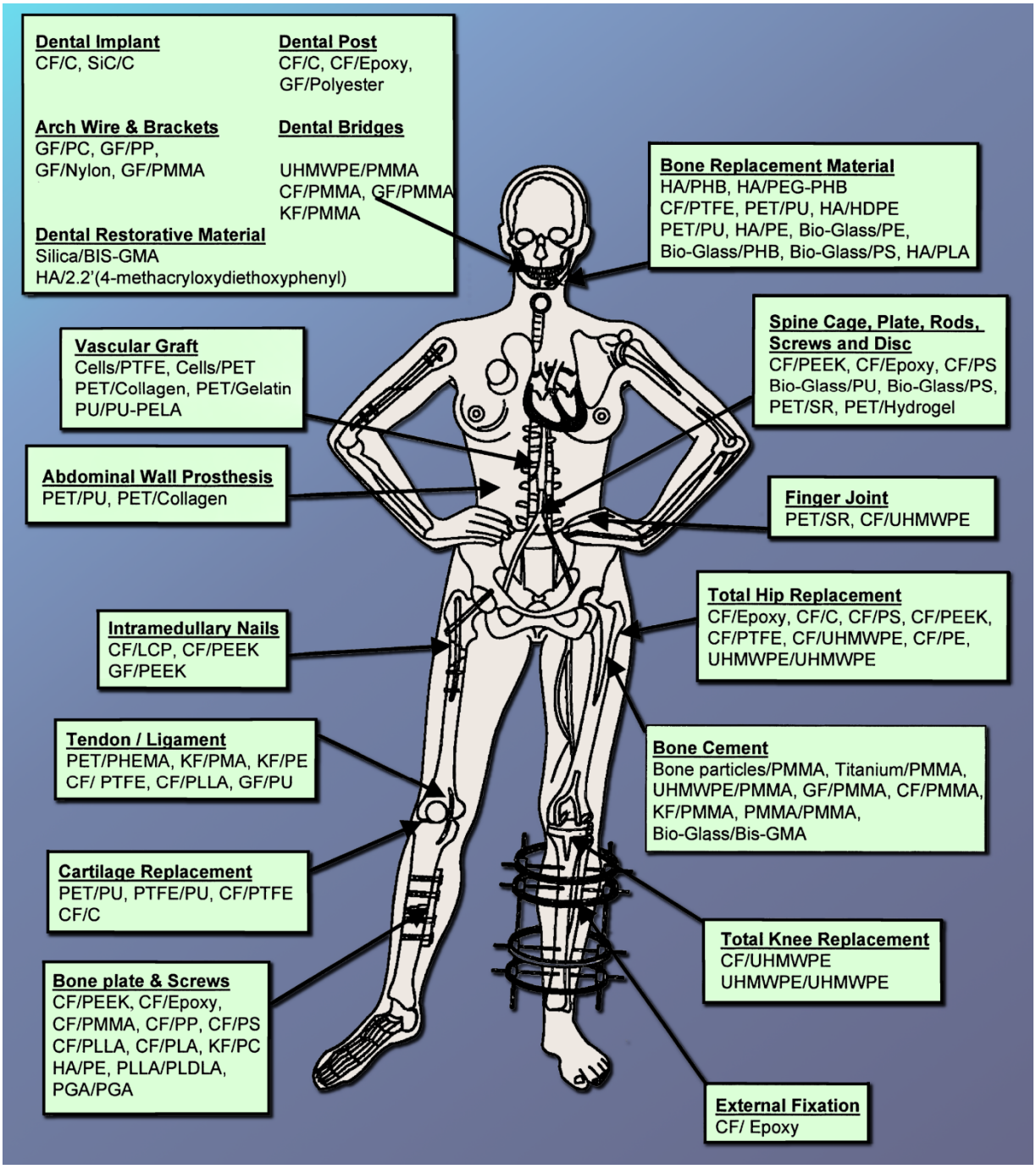

Figure 2.3: Various applications of different composite biomaterials [22]

http://www.sciencedirect.com/science/article/pii/S0266353800002414

2.3.1. Metallic devices

First generation biomaterials were selected to be as bio-inert as possible and thereby minimize formation of scar tissue at the interface with host tissues. Traditional metal implants primarily included devices such as pins, screws, staples, plates. Metal plate-screw systems are fixation materials that have been used for a long time commonly in plastic and orthopaedic surgery. These implants are typically fabricated of metals such as stainless steel, titanium and its alloys, and other materials. Despite their widespread use, a relatively consistent set of problems or issues have been identified. These materials are stiffer than bone and offer the potential for stress shielding with resultant bone resorption and weakening .and also second surgery is necessitate for remove the metal implant [8][23][24].

2.3.2. Bioglass

Bioceramics and bioactive glasses are biomaterials which enjoy an extensive acceptability in bone healing applications. A common characteristic of bioactive ceramics or glasses (or glass–ceramic materials) is that their surface develops a biologically active hydroxyl carbonate apatite layer which bonds with collagen fibrils. These reactions eventually result in a mechanically strong interfacial bonding which can resist substantial mechanical force.

Hydroxyapatite (HA) is a natural component of bone that can also be synthetically processed into powders, solids and porous scaffolds. The first bioactive glasses, a set of completely synthetic materials with bone-bonding ability, were developed by Larry Hench [25] within the Na_2O–CaO–P_2O_5–SiO_2 system. The composition having the highest level of bioactivity was named as 45S5 Bioglass® (Figure 2.4), being composed by $24.5Na_2O$–$24.5CaO$–$6P_2O_5$–$45SiO_2$. This material exhibits a number of limitations (poor sintering ability and high crystallization trend upon heat treatments, high solubility/degradability and poor processing properties in water, low mechanical strength and toughness, etc.). Since the molecular structure of glasses plays a crucial role in deciding their bioactivity, understanding their structural features is considered to be an essential requirement for designing new glasses with improved chemical durability and tailored biodegradability for specific applications.

All of bioactive materials form a mechanically strong interfacial bond with bone. The strength of the bond is generally equivalent to or greater than the strength of the host bone, depending on test conditions. Thus, all of these materials have excellent biochemical compatibility (bioactivity). However, their flexural strength, strain-to-failure, and fracture toughness is less than bone and their elastic moduli are greater than that of bone. It means that most bioactive materials have a less than optimal biomechanical compatibility when used in load- bearing applications. An approach to solving this problem is using these materials as particulates and coatings, or in low load bearing applications [26][27][28][25].

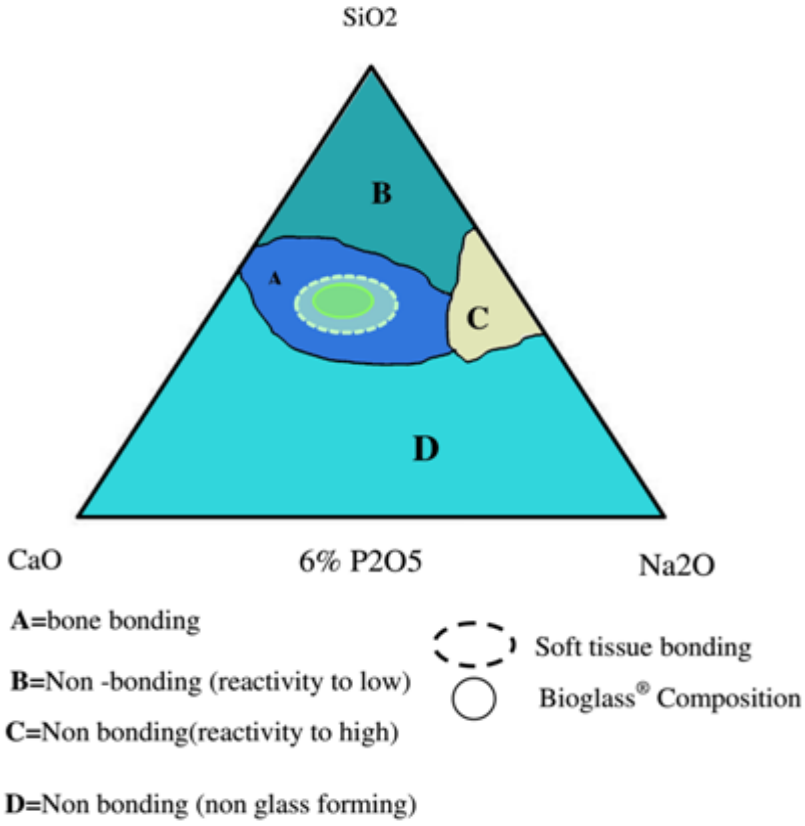

Figure 2.4: Simplified ternary phase diagram of 45S5Bioglass®[27]

2.3.3. Bioresorbable polymers in trauma and bone surgery

The clinical use of synthetically produced polymers started in the 1960s [29]. Compared to metallic or ceramic materials, the advantages of polymeric biomaterials are the ease of manufacturing of products with various and complex shapes, reasonable cost and their availability in a wide range of physical and mechanical properties. For certain applications, it may also be an advantage that the stiffness of polymeric materials is much closer to the stiffness of bone in contrast to metals or ceramics [30].

During the last few decades interest in resorbable materials, i.e. biomaterials which degrade *in vivo* to non-harmful by-products has been steadily increasing [31]. Degradation products of such materials are usually present in the body as metabolites or constituents of the tissues. The early application of bioresorbable polymers almost exclusively for sutures [32] is now widely expanded. Implants for trauma surgery (pins, screws, plates, dowels, anchors, membranes drug carriers [33], and tissue-engineered implants are typical examples. Nevertheless, quite a number of implants made from resorbable polymers are commercially available nowadays. Pins and screws are used for the fixation of bone flakes in limited load bearing fractures; small plates and screws are applied in craniofacial surgery; interference screws and staples are used in knee surgery for the re-attachment of ligaments.

Tissue reaction to resorbable polymeric implants is much dependent on the material chemical composition, its degradation rate and toxicity of degradation products. Physical factors, which affect tissue response to implants include, their shape, physical structure, the mass of the implant, the stress at the implantation site and the micromotions at the implant tissue interface.

2.3.4. Polycaprolactone (PCL) a resorbable polymer

PCL as one of the earliest synthetic polymers renders low mechanical properties which is not sufficient to apply in very high load bearing applications [3]. PCL degradation rate is slower than PGA and PLA and their copolymers (3-4 years) and this property makes PCL an interesting polymer to use in drug delivery systems and other biomedical applications that require slower degradation rates and longer time for injury healing [1][3]. It means that despite poor mechanical properties, slow degradation rate of PCL could be a positive point in many cases.

The sequence of polyesters degradation rates decreases in the following order:

PGA > PDLLA > PLLA > PCL

PCL was selected based on a set of attractive features: it has been approved by the Food and Drug Administration (FDA) to specific applications use in the human body [3][34][35]; is easy to process owing to its interesting thermal behaviour; possesses a number of other relevant properties for the intended applications, including biocompatibility, a relatively slow degradation kinetics in comparison to polylactides. These properties make PCL a suitable matrix for the preparation of long term implantable devices, being compatible with a range of other materials.

Materials synthesized from polymers with high degradation rates will lost their stability in long–term industrial uses very fast. In the case of resorbable screws made of high degradation rate polymers, 80% of strength and 60% of stiffness will lost by 6 weeks. This is unpleasant in terms of screws role to close the fracture gap properly and providing good stabilization and sufficient stiffness [1][3].

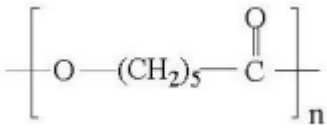

Main chain of PCL [36]

Table 2.1: Mechanical properties of typical polymeric biomaterials

Material	Modulus (GPa)	Tensile Strength (MPa)
Polyethylene (PE)	0.88	35
Polyurethane (PU)	0.02	35
Polytetrafluoroethylene (PTFE)	0.5	27.5
Polyacetal (PA)	2.1	67
Polymethylmethacrylate (PMMA)	2.55	59
Polyethylene terepthalate (PET)	2.85	61
Silicon Rubber (SR)	0.008	7.6
Polysulfone (PS)	2.65	75

2.4. Composite materials and their use in fixation devices

Composite materials are composed of two or more distinct constituent materials or phases on a size scale larger than atomic scale. In comparison to homogeneous materials, composites have plenty of advantages. Composites have the potential to produce hard, strong and light materials, with complex elastic properties.

A single material type does not usually provide the necessary mechanical and/or chemical properties required. Hence, the properties of two or more materials can be smartly combined in a composite material that might exhibit key properties for an intended application. This is the reasoning behind the present research proposal that aims at combining the attractive properties of polycaprolactone (mechanical, biodegradability and non-cytotoxicity) with the excellent bioactivity of a bioglass, FastOs®BG to obtain a composite material with the required properties for the fixation of tendons and bone fractures. The polymer matrix plays a critical role in providing the necessary mechanical stability to constructs. On the other hand, bioactive glasses have the ability to degrade *in vivo* and are ideal candidates for being incorporated in the composite structure to confer them the ability to gradually degrade while offering an active surface for bone growth and the replacement of the implant materials. Provided that the degradation rate of the implant materials and the rate of bone growth match, the required conditions for a strong bond with the living bone tissue are met.

There are many matrix materials and even more filler types which can be combined in countless ways to produce just the desired properties. The physical property of final product significantly alters in compare to those of the initial components.

Size, shape (Figure 2.5), aspect ratio and distribution of reinforcing particles are parameters which can effect on mechanical properties of composite. In the case of polymer matrix composites, the addition of rigid particles to polymers can increase the stiffness, reduce coefficient of thermal expansion (CTE), and improve the resistance to fracture and toughness [8][10][37][38].

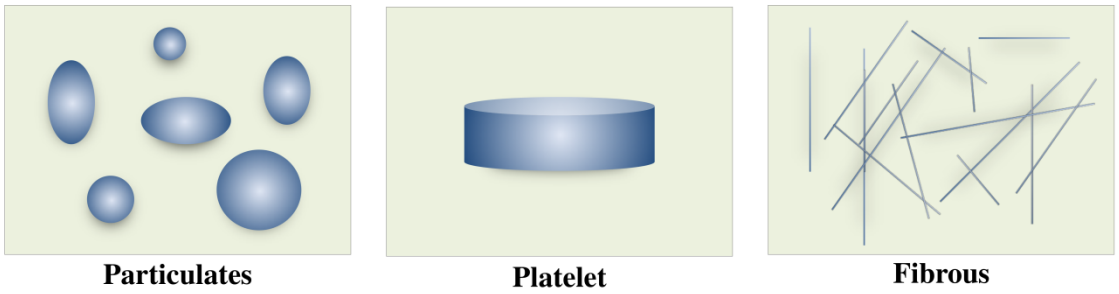

Figure 2.5: Additives morphology in composites

2.5. Effect of particle loading on mechanical properties

2.5.1. Young's modulus

The effects of particle loadings on composite modulus have been studied for various composites. Investigation by Dekkers *et al*. [39] showed that Young's modulus of polystyrene (PS)/glass-bead composites increased almost linearly with glass loading. Studies by Suprapakorn *et al*. [40] showed that the elastic modulus of $CaCO_3$-filled polybezoxazine composite could be increased with increasing filler contents. Wang *et al*. [41] have found that Young's modulus of hydroxyapatite (HA) filled poly-ethylene composites was strongly dependent on particle loading. Similar results for other particulate-polymer composite systems also have been obtained. Studies by Tjong *et al*. [42] showed that tensile modulus of ternary polymer composites: polyamide 6, 6 (PA 6, 6)/poly [styrene-b-(ethylene-co-butylene)-b-styrene] grafted by maleic anhydride (SEBS-g-MA)/glass beads, was enhanced by adding glass beads. Another study by Amdoui *et al*. [43] proved that modulus of epoxy/glass bead composites increased with glass bead volume fraction. Similarly, Yuchun *et al*. [44] found that elastic modulus of nylon 6/silica nano-composites (silica particle size within the range of 50 to 110 nm) increased constantly with increasing silica particle loading. Hence, previous studies proved that embedding rigid particles into a polymer matrix can easily improve the modulus since the rigidity of inorganic fillers is generally much higher than that of organic polymers. The composite modulus consistently increases with increasing particle loading as described by the several models summarised in Table 2.2.

Table 2.2: Theories for elastic modulus

Name	Model	Nomenclature
Einstein's Equation [9]	rigid particles in particulate composites $\mathbf{E_c = E_m (1 + 2.5V_f)}$	$\mathbf{E_c}$ = Young's modulus of composite $\mathbf{E_m}$ = Young's modulus of matrix $\mathbf{V_f}$ = particle volume fraction
Guth model [9][45]	Guth model For spherical particles $\mathbf{E_C = E_p (1 + K_E V_f + 14.1 V_f^2)}$ For non-spherical particles $\mathbf{E_C = E_m (1 + 0.67\alpha V_P + 1.62\alpha^2 V_p^2)}$ assuming $\alpha >> 1$	$\mathbf{E_c}$ = Tensile modulus of the reinforced polymer $\mathbf{E_p}$ = Tensile modulus of the matrix $\mathbf{K_E}$ = Einstein coefficient $\mathbf{V_f}$ = Reinforcement volume fraction $\boldsymbol{\alpha}$ = Reinforcement aspect ratio
Halpin and Tsai model [13][45]	Composite contain spherical particles $E_C = E_m \left(\frac{1 + ABV_P}{1 - BV_P}\right)$	A=function of the particle shape and matrix Poisson ratio B= related to the modulus of the particle and matrix E_c = Young's modulus of composite E_m = Young's modulus of matrix
Kerner [9]	$E_c = E_m \left(1 + \frac{Vp}{Vm}\frac{15(1-\nu m)}{(8-10\nu m)}\right)$ For $E_p >> E_m$	ν_m = poisson ratio
Nielsen [9]	Based on Halpin -Tsai & Kerner model $E_c = E_m \left(\frac{1 + ABV_P}{1 - B\delta V_P}\right)$	δ = depends on particle packing fraction A= factors such as geometry of filler and passion ratio of matrix B = relative moduli of filler and matrix phase

2.5.2. Mechanical strength

The strength of a material is how well a material can resist being deformed from its original shape. The maximum stress that the material can sustain under uniaxial tensile loading is defined as strength [46]. For micro- and nano-particulate composites this relies on the effectiveness of stress transfer between matrix and fillers. Factors like particle size, particle/matrix interfacial strength and particle loading can significantly affect the composite strength [6][9][47].

There are different studies regarding to the effects of particle size and particle-matrix interfacial adhesion. But investigations regarding the effect of particle loading on composite strength showed various trends due to the interplay between particle size, particle-matrix interfacial adhesion and particle loading. These factors cannot always be separated, for instance the study on the effect of spherical filler particle size (various range of size in µm and nm scale) by Chacko *et al*. [48] on tensile strength of the polypropylene (PP)/$CaCO_3$ composites proved that strength of micro particle filled composites decreased with particle content. But another study by Maazouz *et al*. [49] regarding to effect of particle size on tensile strength of epoxy composites filled with spherical silica particles with different particle contents also another research by Pukanszky *et al*. [50] regarding to effect of $Mg(OH)_2$ loading with different particle size on tensile strength of Ethylene Propylene Diene Monomer /Magnesium hydroxide composites ($Mg(OH)_2$/EPDM) showed the reverse results. For instance in micro-size, strength increases with particle content. Beside particle size and loading, the particle/matrix interfacial adhesion also significantly affects the strength of particulate composites. So materials response contradictions could be justify by these characteristics [51][45].

Ou *et al*. [44] studied tensile strength of nylon 6 nano-composites filled with modified and unmodified silica (SiO_2) particles within the size range of 50 to 110 nm. Results proved that for untreated particles the strength decreases only marginally with increasing particle content. However, for modified compositions, good particle dispersion and strong polymer/silica interface adhesion caused effective stress transfer. Therefore, the composite strength was increased. When silica content was above 5 wt.% particle aggregation occurred, leading to degradation of composite strength as the particle content increased.

Researches by Tjong *et al*. [42] showed that tensile strength of the ternary polymer composites, polyamide 6, 6 (PA 6, 6)/maleated poly [styrene-b-(ethylene-co-butylene)-b-styrene] (SEBS)/glass beads, was reduced by addition of glass beads (GBs).

Also, the effects of various glass bead loadings and different rubber contents on strength of hybrid particulate epoxy composites with were investigated by Maazouz *et al*. [49]. Results showed an increasing trend in tensile strength with increasing added amounts of glass beads (within the size range of 3 – 70 μm).

Various trends have been observed for the effects of particle loading on composite strength. Besides particle loading, these observations revealed that particle size and particle/matrix interfacial adhesion also play important roles in determining the strength of particulate composites. The interplay between particle size, particle matrix interfacial adhesion and particle loading determines the resulting mechanical properties [45][52].

2.5.3. Theories for ultimate strength of composite materials

Although the main factors that determine the fracture behaviour strength of a composite (size and shape of the inclusions, volume fractions of polymer and filler, and particle-matrix interfacial bonding have been identified [6][12][52], the theoretical models for predicting strength behaviour of filled systems are not much developed. In some cases the theoretical models neglect several parameters, so the predictions often fail giving a good fit to experimental data. Table 2.3 presents some theoretical models proposed for predicting the mechanical strength of composite materials.

The application of the equations presented in Tables 2.2 and 2.3 implies knowing the parameters involved in each one. They might include geometrical features of the particles and the strength of the interfacial adhesion between polymeric/inorganic phases. In the present work the filler is in the form of isometric particles. On the other hand, the bonding between matrix and filler is not expected to be strong due to the hydrophobic nature of polymer matrix and the relatively hydrophilic character of FastOs®BG Di–70 bioglass.

Table 2.3-Theories for predicting the mechanical strength of composite materials

Name	Model	Nomenclature
Basic (simplest) equation [9][13]	Poorly bonded particles. Stress cannot transfer from matrix to filler $\delta_c = \delta_m (1-v_p)$	δ_c = composite strength δ_m = matrix strength v_p = particle volume fraction
Modified basic model [9]	Poor bond between matrix and filler, absence of stress concentration at the particle matrix interface $\delta_c = \delta_m (1- a v_p^b)$	**a, b** = constant (depending on particle shape and arrangement in the composite)
Nicolais & Nicodemo [13]	No adhesion between filler and polymer, all load is sustained only by the polymer $\delta_c = \delta_m (1 - 1.21 v_p^{2/3})$	For simple geometric consideration which gives lower strength bond of composite (upper bond is equal to strength of polymer matrix). Strength will be an intermediate between upper and lower bonds.
Jancar et al. [13]	Nicolais &Nicodemo modified model $\delta_c = \delta_m (1 - 1.21 v_p^{2/3}) S_r$	S_r = strength reduction factor 0.2 to 1.0 for low and high volume fraction.
Leidner-Woodhams [9]	Spherical particles in elastic matrix For good interfacial adhesion: $\delta_c = (\delta_a + 0.83\tau_m) + \delta_a k (1- v_p)$ for no interfacial adhesion: $\delta_c = 0.83\, \delta_{th}\, \alpha\, v_p + d\, \delta_m (1- v_p)$ or $\delta_c = 0.83\, pf\, v_p + r\, \delta_m (1- v_p)$	δ_a = strength of interfacial bond δ_m = (ultimate) matrix strength τ_m = shear strength of matrix **k**= stress concentration factor ***d***= parameter depend on particle size δ_{th}= thermal compressive stress α = coefficient of friction p = pressure f = friction coefficient **r** = relative change in matrix strength due to presence of filler.

CHAPTER 3

3. MATERIALS AND METHODS

This work aims at developing composite materials comprising a polymeric PCL matrix filled with different proportions of a bioactive glass (FastOs®BG Di–70) powder and study the effects of the added amounts of filler on the mechanical properties of final composites.

Different shaping methods (hot pressing, injection moulding) were applied to prepare specimens for assessing the mechanical properties under compressive, tensile, oscillatory and torsional testing modes, following whenever possible the standard specifications for each type of test.

3.1. Materials

The starting materials to fabricate the resorbable composites included a semi-crystalline (56%) aliphatic thermoplastic polycaprolactone (PCL) powder with an average molecular weight of 50,000 g mol^{-1}, a low melting point of 58–60ºC, and a glass transition temperature (T_g) of approximately −60ºC, as matrix; and an alkali-free bioactive glass powder (FastOs®BG Di–70) as filler.

The FastOs®BG Di–70 was selected from a series of alkali-free bioactive glass compositions designed in the system diopside (hereafter referred to as Di) – tricalcium phosphate (hereafter referred to as TCP), generically designated as $Di_{(100-x)}$–TCP_x [10]. The selection of x = 30 wt. % in present case was due to the fact that this was shown to exhibit the highest bioactivity among this series of phospho-silicate glass compositions studied.

3.1.1. Preparation of FastOs®BG Di–70 bioactive glass

The synthesis included high-purity powders of SiO_2 (purity >99.5%), $CaCO_3$ (>99.5%), $MgCO_3$ (BDH Chemicals Ltd., UK, purity >99.0%), ZnO (Sigma Aldrich, Germany, 99.9+%), $NH_4H_2PO_4$ (Sigma Aldrich, Germany, >99.0%), as described elsewhere [10]. A homogeneous batch

(~100 g) obtained by ball milling, was preheated at 900ºC for 1 h for decarbonisation and then melted in a Pt crucible at 1570ºC for 1 h in air. The molten glass was poured in cold water to obtain a frit, which was then dried and milled in a high-speed agate mill, resulting in a fine glass powder with mean particle size within the range of ~38 μm (determined by light scattering technique; Coulter LS 230, Beckman Coulter, Fullerton, CA; Fraunhofer optical model). The amorphous nature of glasses was confirmed by X-ray diffraction (XRD) analysis (Rigaku Geigerflex D/Max, Tokyo, Japan; C Series; Cu K_α radiation; 2θ angle range 10 – 80; step 0.02 s^{-1}).

The characteristics of the as obtained FastOs®BG Di–70 bioactive glass powder are reported in Table 3.1.

Table 3.1 - Characteristics of FastOs®BG Di–70 bioactive glass

Composition (mol%)	36.52 CaO−19.24 MgO−38.48 SiO_2−5.76 P_2O_5
Average particle size (μm)	38
Density (g cm^{-3})	2.94±0.01
T_g (Cº)	757
Glass ultimate strength (MPa)	103.5±5.1

3.1.2. Preparation of PCL/FastOs®BG Di–70 composites

The starting materials were combined in different weight proportions, as reported in Table 3.2, by melting and stirring at suitable temperatures within the range of 60–95ºC to obtain a kind of feedstock pellets (Figure 3.1) to fabricate the resorbable composites by different processing techniques, plastic forming under a pressure of 110 MPa, and also by injection moulding.

Figure 3.1: Composites feedstock

Composites with different filler volume fractions were prepared by hand blending method. For this purpose proper PCL and BG powder was measured properly for each composition. Mixed composite powders were placed afterward in the oven for 30 minutes. For pure PCL the temperature of the oven was adjusted on 60ºC. Gradually higher temperatures were required as the proportion of FastOs®BG Di–70 was increased.

Table 3.2: Compositions of PCL based composites

Sample Code	Filler fraction		Density of composite (g cm^{-3})
	(wt.%)	(vol.%)	
PCL–BG00	0	0.00	1.14
PCL–BG20	20	8.84	1.29
PCL–BG30	30	14.25	1.39
PCL–BG40	40	20.54	1.51
PCL–BG50	50	27.94	1.64
PCL–BG60	60	36.77	1.80

Table 3.3 indicates the temperature values used for the preparation of the feedstock and of the composite specimens for compressive tests. The specimens shaped by injection moulding for tensile and DMA tests were prepared from the same feedstock under specific conditions of temperature and pressure applied to immediately before with different proportions of filler.

Table 3.3: Oven's temperature for preparation of feedstock

Composite codes	Ovens temperature (°C)
Pure-PCL	60
PCL-BG20	65
PCL-BG30	70
PCL-BG40	75
PCL-BG50	85
PCL-BG60	95

The experimental conditions used to prepare the injection moulded samples for tensile and DMA tests have to be varied according to the proportions of the components in the composite mixtures, as reported in Table 3.4.

Table 3.4 - Experimental conditions used in injection moulding

Composition Name	Temperature (ºC)		Pressure (bar)	Time (s)
	Cylinder	Mould		
PCL-BG00	90	40	450	15
PCL-BG20	95	40	450	15
PCL-BG30	98	40	480	15
PCL-BG40	105	40	500	15
PCL-BG50	108	40	520	15
PCL-BG60	110	43	600	15

3.2. Characterization methods

3.2.1. Tensile tests

Tensile testing was conducted in accordance with ASTM standards D638. (ASTM D638 is a test method which covers the determination of the tensile properties of unreinforced and reinforced plastics in the form of standard dumbbell-shaped test specimens when tested under defined conditions of pre-treatment (temperature, humidity, and testing machine speed). Also this test method and ISO 527-1,-2 are technically equivalent [53]. Tensile specimens were tested using a displacement controlled Shimadzu tensile testing machine at a displacement rate of 50 mm. min^{-1}. Each specimen was loaded until the maximum allowable plastic deformation (before rupture). This test method includes also the option of determining Poisson's ratio at room temperature.

Tensile properties may vary with specimen preparation and with speed and environment of testing. It has underlined that the mechanical properties of a material cannot be reported without also referring to the preparation method of the samples and to the testing conditions used. Hence, when comparative tests of materials per se are desired, the greatest care must be exercised to ensure that all samples are prepared under exactly the same way, unless the test is intended to assess the effects of the experimental variables used for sample preparation [52] [53].

By applying a tensile stress (σ) along the longitudinal axis of the specimen, it elongates in a way that depends mainly on the type of solicitation, the nature of the material (i.e. chemical composition, crystal grains density, presence of crystal defects, etc.) and the temperature. By determining strain–stress curve, the mechanical behaviour of a given material can be appraised. Consequently, where precise comparative results are desired, these factors must be carefully controlled.

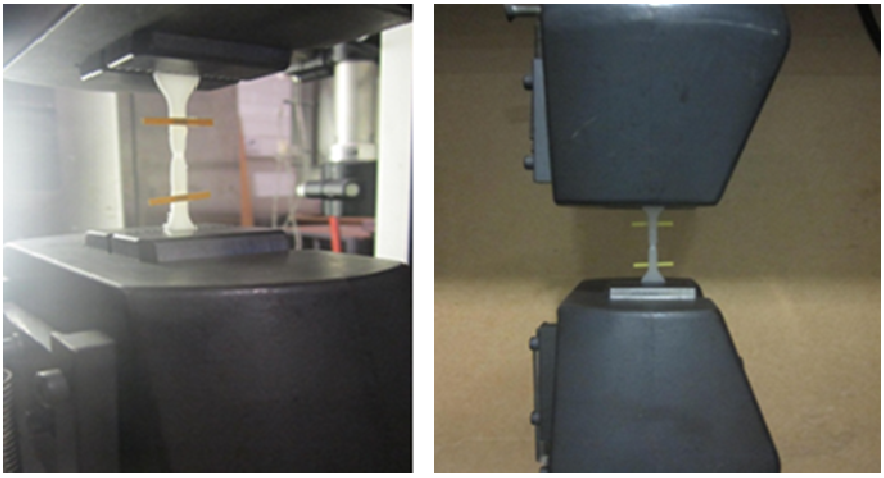

Figure 3.2: Tensile specimen edges gripped between tensile machine hands

NOTE: Tensile properties may provide useful data for plastic engineering. However, because of the high degree of sensitivity exhibited by many plastics to rate of straining and environmental conditions, data obtained by this test method cannot be considered valid for applications environments widely different from those of this test method. In cases of such dissimilarity, no reliable estimation of the limit of usefulness can be made for most plastics.

3.2.1.1. Tensile test procedure

1. Dumbbell-shaped samples of each composition were prepared by injection moulding method.
2. Four specimens of each composite were chosen. Care is to be taken to ensure that the specimens did not have any notching or cracks from manufacturing or any surface defects that would adversely affect the tensile tests.
3. Before loading the specimens in the Shimadzu machine, the computer system connected to the machine was set up by inputting the necessary information of gauge length and width of the specimen. The computer system was then prepared to record data and output necessary load-deflection graphs. It is necessary also to calibrate video extensometer and select appropriate operating conditions.
4. Dumbbell-shaped specimen is gripped at its two ends and is pulled by subjecting to an axial load to elongate at a determined rate of 50 mm per minute, until deformation (Figure 3.2).

5. By performing the test to each specimen, the data was recorded electronically in text files and the load-deflection curve was shown on the computer screen as a visual representation of test results.

During the test, the applied load causes a gradual deformation (elongation) of the material. The results were recorded and load-stroke curve was plotted by software. So the tensile behaviour of material could be obtained. An engineering and real stress-strain curve can then be constructed from this load-elongation curve by making the required calculations. The mechanical parameters could be fined by studying these curves.

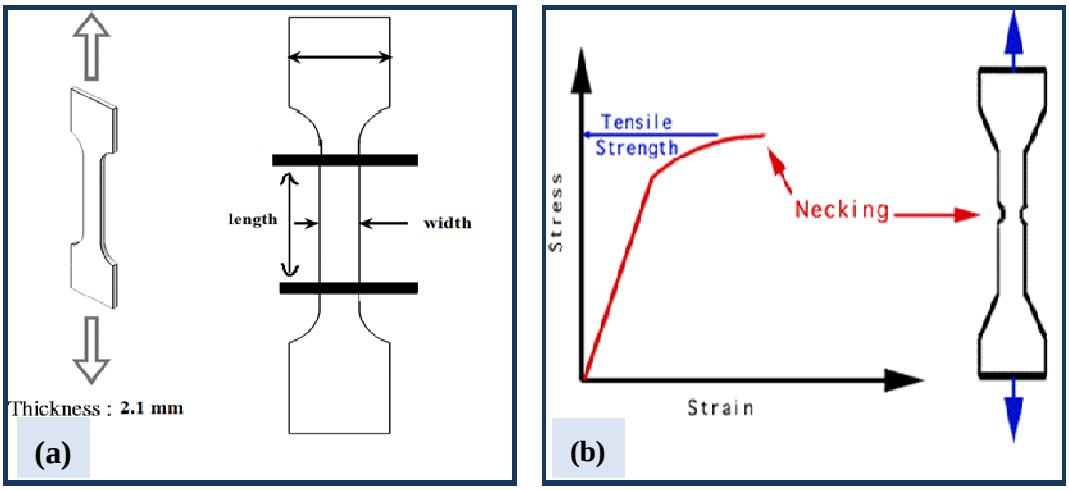

Figure 3.3: Dimensions of a dumbbell shape sample for tensile test (a) -Ultimate tensile strength and necking point in a sample (b)

3.2.2. Compressive test

A compression test is a method for determining the behaviour of materials under a compressive load. Compression tests are conducted by loading the test specimen between two plates and then applying a force to the specimen by moving the crossheads together. Compression test is just opposite in nature to tensile test. It means nature of deformation is quite different from that in tensile test. Compressive load tends to squeeze the specimen. It is apparent, therefore, that in contrast to tensile stresses, which open cracks, compressive stresses tend to close them. This could conceivably enhance the tensile strength [53][54].

3.2.2.1. Experimental procedure

The method by which the compression test shall be conducted is defined in ASTM D695 type 2a. This is suitable method to determine compressive properties of rigid plastics. In this work uniaxial compression tests have been done using AG-IS SHIMADZU (10KN) machine to determine elastic limit of different composites. The accuracy of the uniaxial compression test depends on the planarity and the parallelism of the contact area. Planarity and parallelism of the two metallic platens that compress the samples have been checked. Great care was taken to ensure that the end faces of the test specimens were smooth and plane-parallel. It has been realized also that a material cannot be tested without also testing the method of preparation of that material. Hence, when comparative tests of materials per se are desired, the greatest care must be exercised to ensure that all samples are prepared in exactly the same way, unless the test is to include the effects of sample preparation. Similarly, for comparisons within any given series of specimens, care must be taken to secure the maximum degree of uniformity in details of preparation, treatment, and handling.

It has been reported in most of compressive tests that the geometrical conditions of the test are important. Specimen alignment plays an important role in achieving even load distribution, which contributes to the consistency of the results. The ratio between the initial length L_0 and the diameter D of the sample is a pertinent parameter. The standard compression test specimen is a cylinder having an L_0/D ratio of 2 [55]. This geometry condition is also suitable for simulation of screws.

Therefore, in the present work, care was taken in order to have all testing specimens made with dimensions and size ratio specified the standard prior to testing. The specimens were prepared as described below:

1. Cylindrical shaped samples were obtained by pressing around 6 g of composite feedstock in the preheated cylindrical mould with diameter of 1.32 cm under a pressure of 110 MPa (see feedstock preparation procedure explained previously in pages 22-23).

2. Diameter and height values for each sample were measured properly by Vernier callipers.

3. Each specimen was placed centrally between the two compression plates such that the centre of moving head was vertically aligned with the centre of the specimen.

4. For each sample, the initial load was firstly adjusted to zero. Then, load was applied on the specimen by movable head of the machine at the rate of 1.3 mm per minute until the specimen height became half of the initial height in order to limit the compressive test to approximately the elastic deformation range of the sample (Figure 3.4).

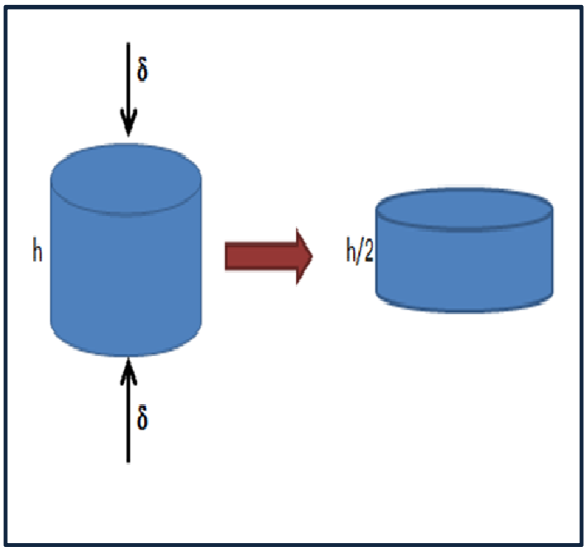

Figure 3.4: Schematic deformation of pellet samples under compression

3.2.3. DMA test

DMA (Dynamic Mechanical Analysis) can be simply described as: applying an oscillating force to a sample and analysing the material's response to that force. In this technique a small deformation is applied to a sample in a cyclic manner. This allows the materials response to stress, temperature, frequency and other values to be studied.

Dynamic Mechanical Analysis has become more popular because of their significant properties and ability to provide information about materials in particular polymers. As a technique, DMA is sensitive for the characterization of polymers of similar chemical compositions, as well as detecting the presence of moderate quantities of additives. DMA gives information about rheological and thermal

properties of polymers. Rheology is very sensitive to small changes of the material's polymer structure thus is an ideal method for characterization of polymers [25][56].

In this work by using DMA test, mechanical properties and efficacy of the filler volume fraction on stiffness and elastic behaviour (Young's modulus) of the material was investigated. It has been proved that small dimensional changes often have large consequences on the final results of DMA test, so it is important to have samples with the same geometry in this test. Namely, it is important that the opposite sides of the specimen should be parallel and perpendicular of the neighbouring sides. Moreover, there should be no nicks or narrow parts along the testing specimen.

3.2.3.1. Experimental procedure

Frequency scans and frequency dependencies are probably the least used and the most powerful techniques in DMA. It represents a powerful probe of material properties that should be in any testing laboratory. Applying different frequencies to the material gives an idea about how it will respond to different conditions. In this work frequency test performed using single cantilever bending deformation mode by Triton technology machine (Tritec 2000 DMA model)(Figure 3.5a). Temperature held constant at 37ºC (body temperature). Samples were prepared by injection moulding method (Table 3.4) and cut into rectangular shapes with precise dimensions of length and width. The strain control tolerance factor of 0.02 mm was set and the experiments were conducted within the frequency range of 0.01 Hz to 1 Hz. Young's modulus, loss factor (Tan delta) and loss modulus were obtained directly from software. Storage modulus and efficacy could be indirectly obtained by theoretical formulations.

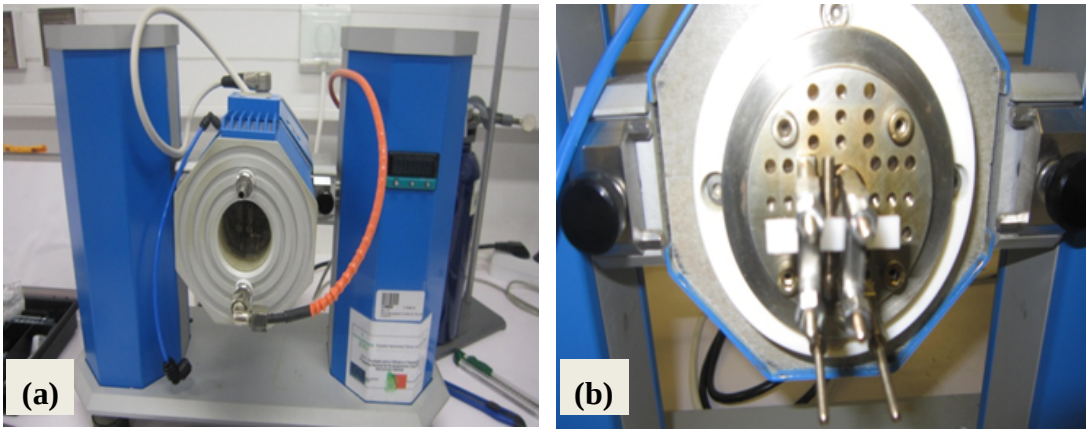

Figure 3.5: (a) DMA test machine (Triton technology machine-Tritec 2000 model; (b) Rectangular shape samples gripped between machines arms

3.2.4. Torsion test

There are different applications for bioresorbable polymeric composites. Polymeric reinforced composites are increasingly used in structural applications. Bioresorbable screws are one of these applications (Figure 3.6). The materials used in this case should require not only adequate strength but also be able to withstand torque in operation. In solid mechanics, torsion is the twisting of an object due to an applied torque, therefore is expressed in **N·m** (Newton Meter).

Torsion test is a method usually used for determining shear strength and to study the plastic flow in materials. It is not as universal as tensile test and does not have unique standardized testing procedures.

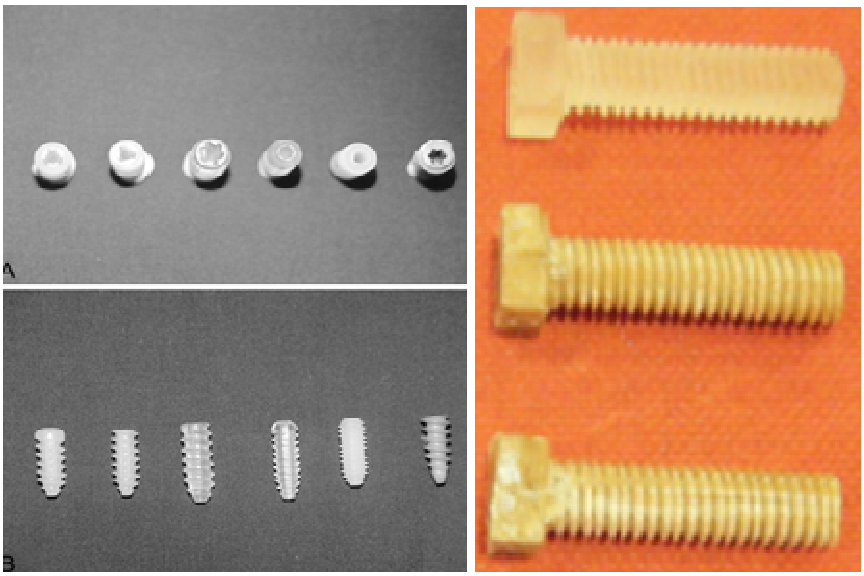

Figure 3.6: Geometry of different types of bioresorbable screws [61]

3.2.4.1.Experimental procedure

Composites with different proportions of FastOs®BG Di–70 were prepared by the hand blending method. For this purpose polymer powder and bioglass power were mixed properly and placed in the rectangular shape aluminium mould. The mould has kept in an oven for 40 minutes at selected temperatures within the range of 70ºC (for pure PCL) up to 90ºC for composite samples. There was a need of gradually increasing the temperature with increasing proportions of FastOs®BG Di–70 BG in the composite. The mould was placed in automatic press and the shaping was performed under an applied load of 400 kg for 3 s. Afterwards, the mould was immersed in cold water and the specimens extracted from it. Three different compositions where selected among all six initially tested ones. Moduli of rigidity (shear modulus) of the composites were investigated by applying torsional test. For this purpose three rectangular shaped samples of each composition were prepared and tested. Length, width and thickness of each sample were measured by Vernier (Figure 3.7).

Figure 3.7: Geometry of samples

In order to study the response of materials under a torsional force, the torsion test was performed by mounting the specimen onto a Shimadzu torsion testing machine. Both ends of the rectangular specimen were tightened to rectangular sockets in which one is fitted to a torque shaft and another is fitted to an input shaft as shown in the photograms of Figure 3.8.

The twisting moment was applied by turning the input segment. At the initial stage, the applied load on the sample was adjusted on zero. Afterwards, the force was gradually increased at a rate of 50 mm min^{-1}. The stroke *versus* force graph was gradually drawn by the software while load was applied to the sample. In this case loading the sample continued up to the end of elastic range within which the elastic deformation of the specimen can be fully recovered upon unloading. However, by applying higher degree of rotation and passing a proportional elastic limit, the specimen starts to deform plastically and will not return to its original shape after unloading (Figure 3.9).

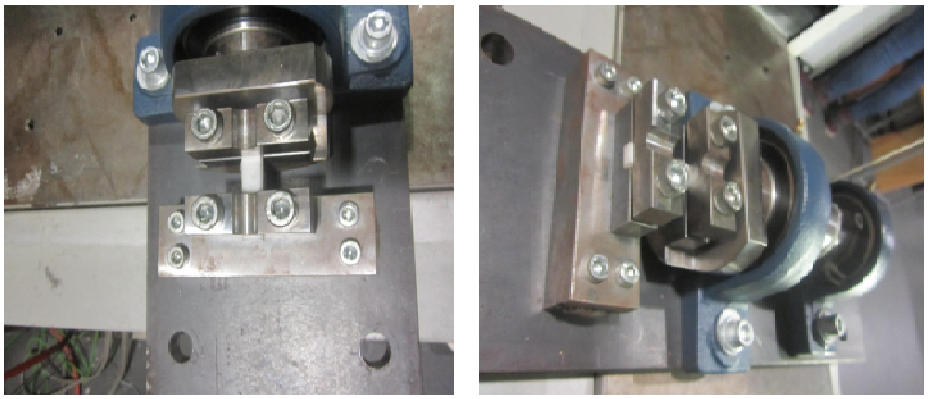

Figure 3.8: Specimens tightened to rectangular sockets fitted to torque shaft in one side and fitted to input shaft on the other side

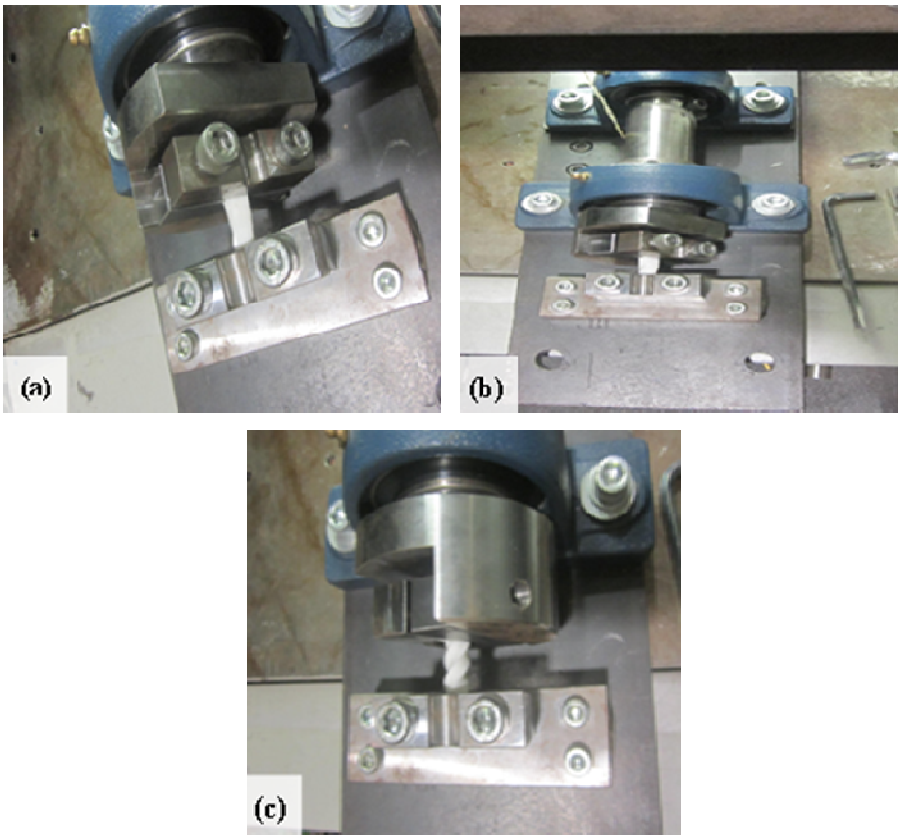

Figure 3.9: Applied torque to the sample in the plastic stage

CHAPTER 4

4. RESULTS AND DISCUSSION

4.1. Tensile tests

The tensile tests data were treated assuming constant volume under deformation as described by Equation 4.1, in which A_0 is the initial cross-sectional area measured prior to running the experiment, L_0 is the initial length, and L_i is the instantaneous length of the specimen at a given moment. From the experiments, the value of Engineering (Nominal) stress can be calculated by dividing the force (F) applied by the machine along the axial direction by its cross-sectional area. Mathematically, it is expressed in Equation 4.2. The Nominal strain values, which have no units, can be calculated using Equation 4.3, where L is the instantaneous length of the specimen.

$A_0 = Initial\ Thickness \times Initial\ Width$

$A = Area\ in\ each\ moment$

$$A = \frac{L_0 A_0}{L_i} \tag{4.1}$$

$$\sigma_N = \frac{F}{A_0} \tag{4.2}$$

$$\varepsilon_N = \frac{L - L_0}{L_0} \tag{4.3}$$

4.1.1. Engineering stress and engineering strain

The data from the tensile tests was plotted on separate graphs according to composites. Each graph shows the engineering stress versus the engineering strain. Figure 4.1 shows tensile test for four samples of pure PCL and the curve representing the average values. Figures 4.2 to 4.5 show the test results for composites with different volume fractions of bioglass filler.

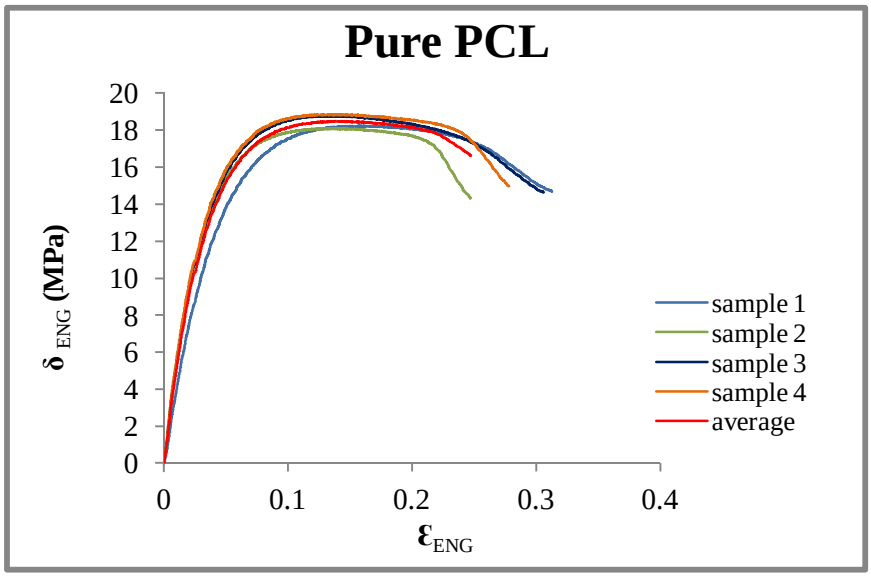

Figure 4.1: Engineering stress-strain results for pure polycaprolactone

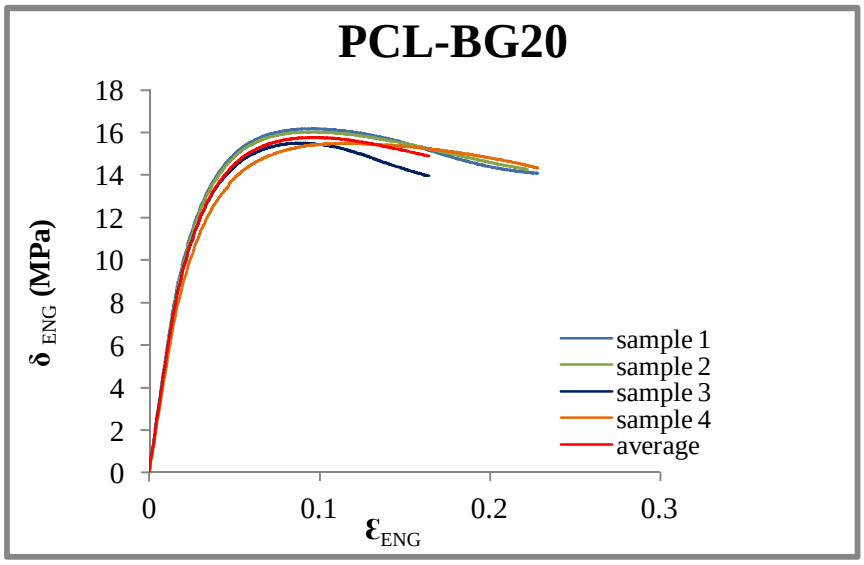

Figure 4.2: Engineering stress-strain graphs for PCL-BG20 composite

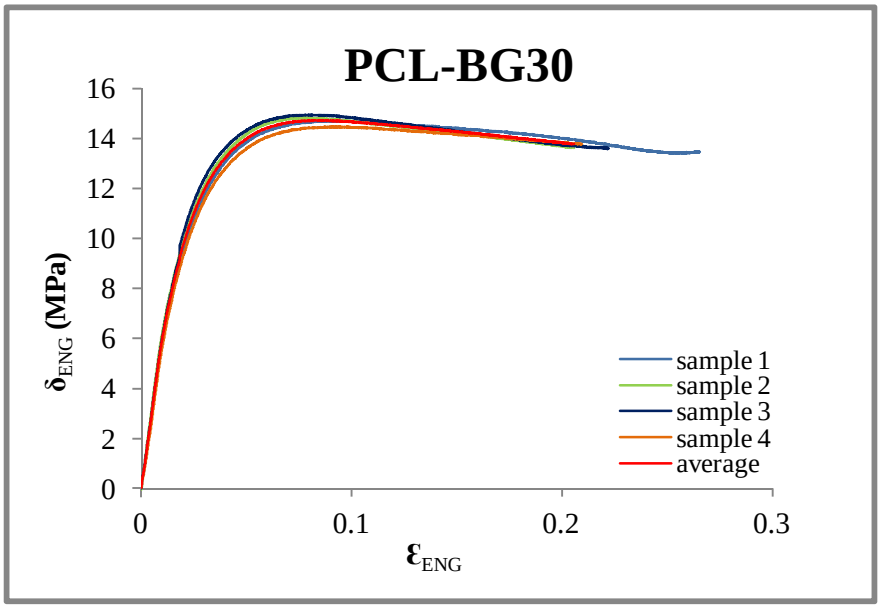

Figure 4.3: Engineering stress-strain graphs for PCL-BG30 composite

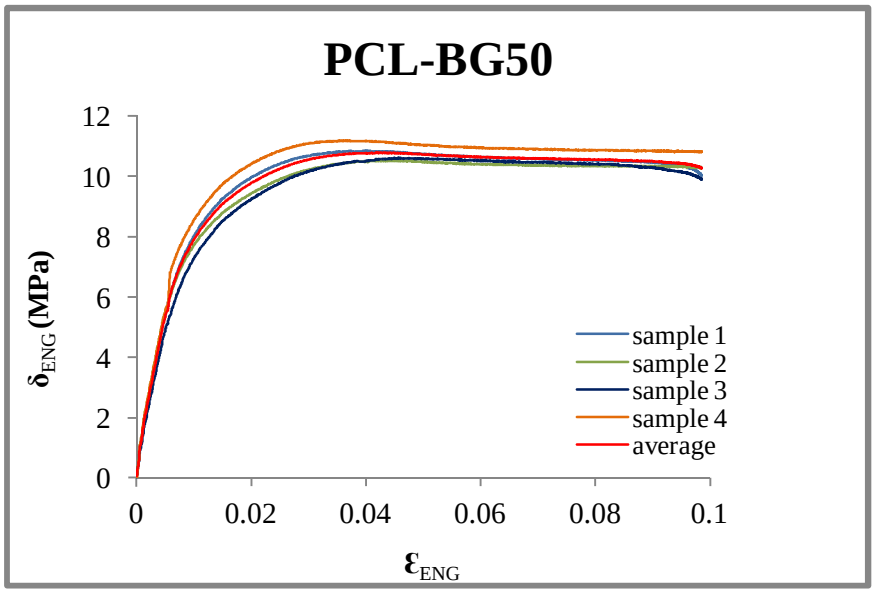

Figure 4.4: Engineering stress -strain graphs foe PCL-BG50 composite

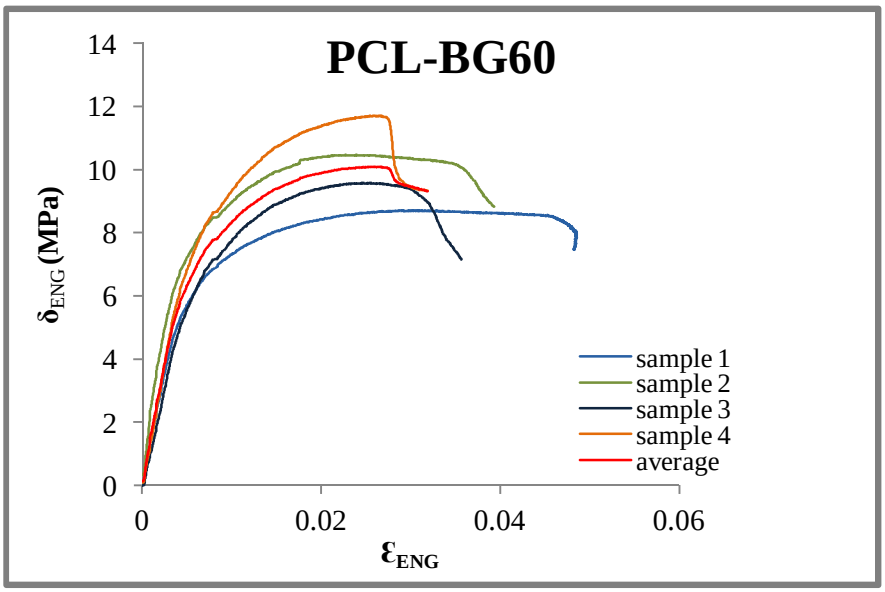

Figure 4.5: Engineering stress-strain graphs for PCL-BG60 composite

4.1.2. True stress and true strain

Theoretically, even without measuring the cross-sectional area of the specimen during the tensile experiment, the "true" stress-strain curve could still be constructed by assuming that the volume of the material stays the same. Using this concept, both the true stress (σ_T) and the true strain (ε_T) could be calculated using Equations 4.4 and 4.5 respectively. In these equations, L_0 refers to the initial length of the specimen, L refers to the instantaneous length and σ refers to the instantaneous stress.

$$\sigma_T = \sigma \frac{L}{L_0} \tag{4.4}$$

$$\varepsilon_T = ln\left(\frac{L}{L_0}\right) \tag{4.5}$$

Figures 4.6 to 4.10 show the true stress *versus* strain variations of four similar samples of each composition. The average stress-strain curve for each set of samples is also plotted for comparison. No significant deviation can be observed among the samples of a given composition. This suggests that a relatively good degree of homogeneity has been achieved during the preparation of the respective feedstock.

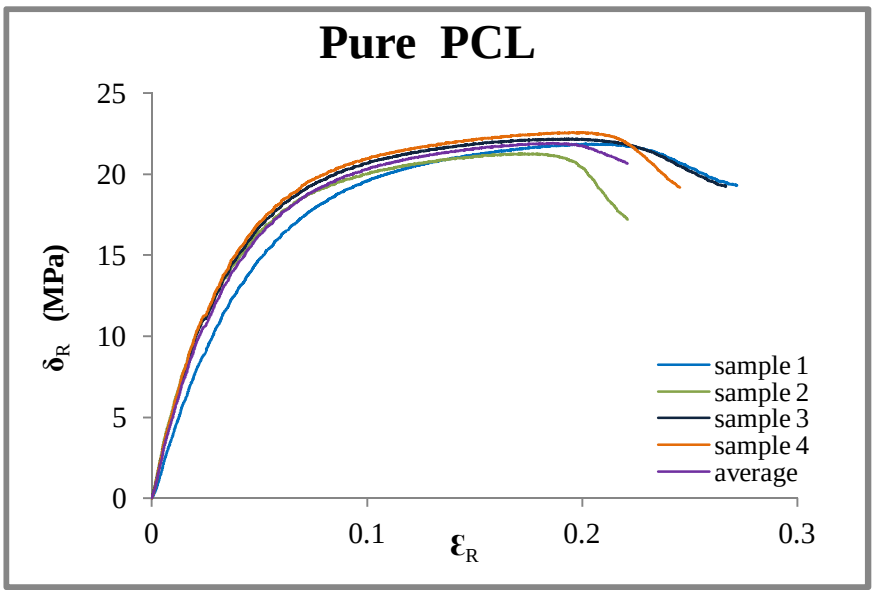

Figure 4.6: True stress-strain graphs of pure polycaprolactone

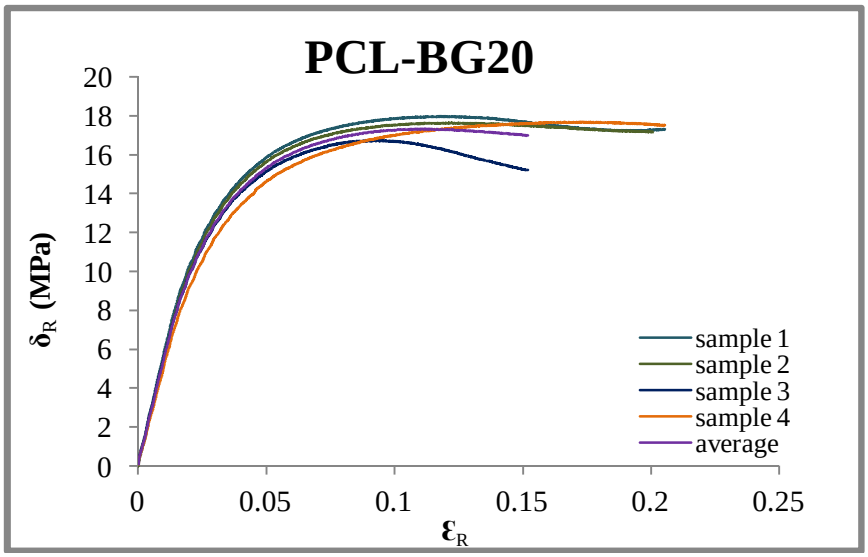

Figure 4.7: True stress-strain of PCL-BG20 composite

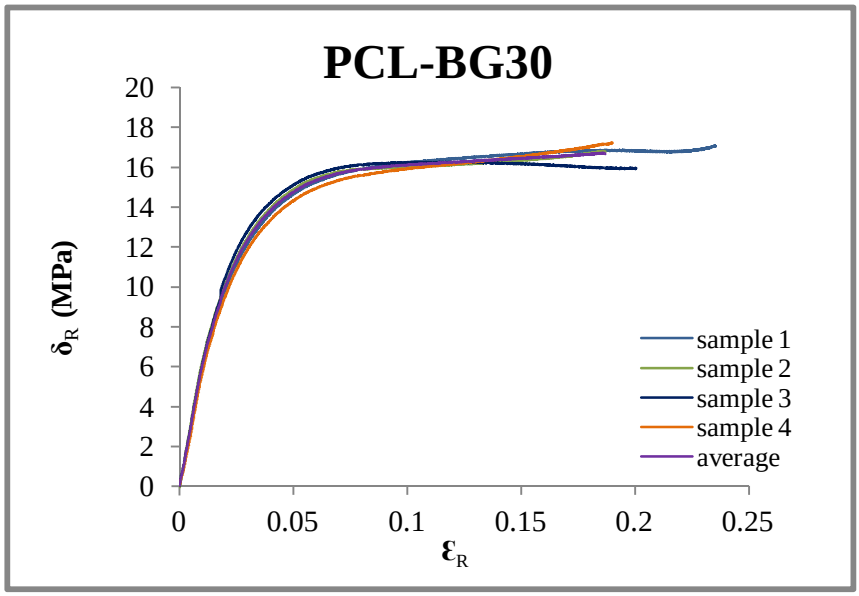

Figure 4.8: True stress-strain graphs of PCL-BG30 composite

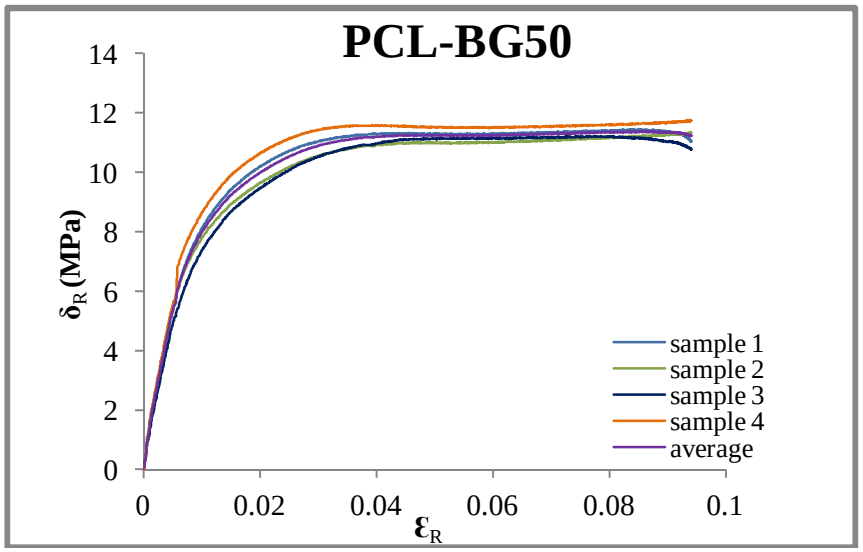

Figure 4.9: True stress-strain graphs of PCL-BG50 composite

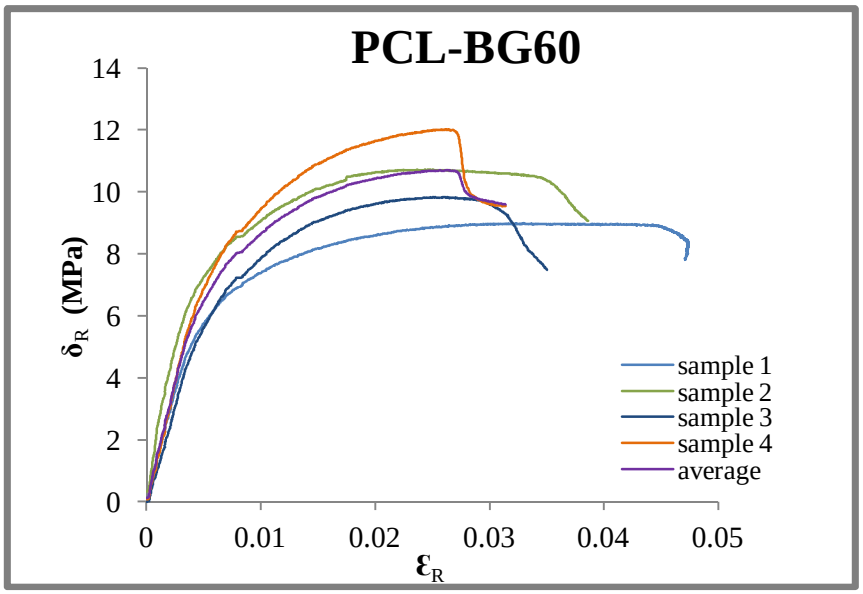

Figure 4:10: True stress-strain graphs of PCL-BG60 composite

4.1.3. Comparison between real and nominal stress-strain results

The engineering stress and strain do not account for the change in cross sectional area, and only accounts for the axial strain in the sample. The true stress and strain account for the change in cross sectional area, and therefore the true stress is higher than the engineering stress.

The elastic modulus and ultimate tensile strength results achieved from graphs presented in Figures 4.6 to 4.10 are presented in Table 4.1. Comparison between real tensile strength values and the nominal ones proves that engineering tensile strength values are lower than the related real ones. The obtained result also show that in the case of composites with higher volume proportion of filler, the difference between real and engineering ultimate tensile strength is less, in good consistency with the less plastic character of the composites having higher volume fractions of bioglass filler. Accordingly, the difference between nominal and real strength is negligible for PCL-BG60.

This phenomenon could be explained by changes in elasticity property of composite. Since higher proportion of bioglass in the composite reduces elastic property of the composite, and stiffer materials with lower elasticity does not show that much changes in terms of cross section area in compare to elastic ones, so for composites containing lower proportions of rigid bioglass, the difference between nominal and engineering strength is significant in compare to composites with higher volume proportion of rigid materials. Figure 4.11 shows the nominal and real stress-strain graphs for all composites. Results for each composition are average of 4 similar samples.

Table 4.1: Real and engineering tensile strength values for all composites

Composite code	Real Tensile Strength (MPa)	Engineering Tensile Strength (MPa)
Pure PCL	21.91 ± 0.76	18.48 ± 0.29
PCL-BG20	17.32 ± 0.36	15.78 ± 0.16
PCL-BG30	16.69 ± 0.03	14.72 ± 0.09
PCL-BG40	14.69 ± 0. 60	12.49 ± 0.64
PCL-BG50	11.36 ± 0.27	10.84 ± 0.25
PCL-BG60	10.69 ± 1.15	10.84 ± 1.27

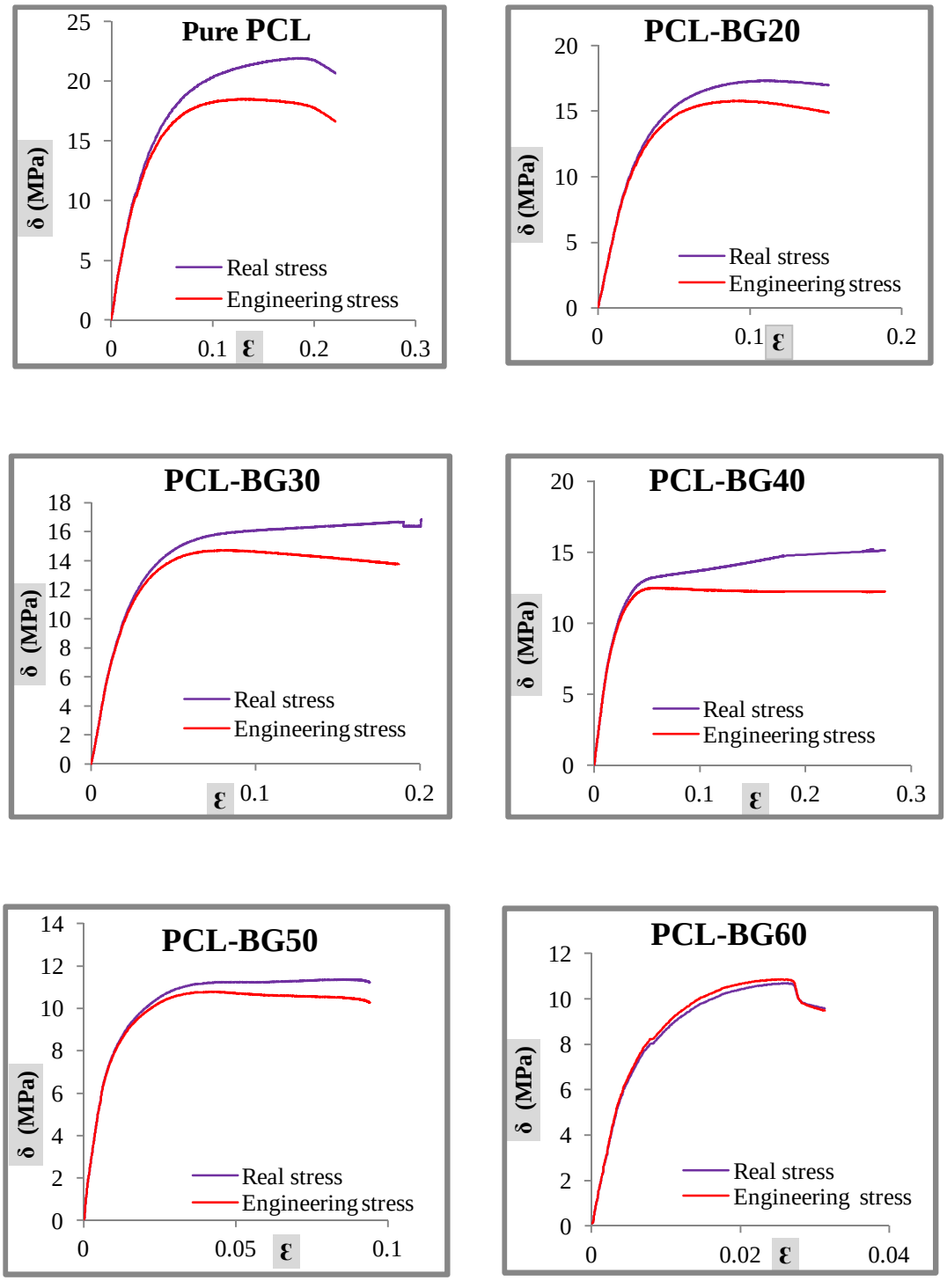

Figure 4.11: Comparison between Nominal and Real stress-strain of all composites

The initial linear part of stress-strain graphs is considered as elastic region. In this range, material shows elastic behaviour and deformations are reversible. The slope of this linear part is taken as the *Young's modulus* which is the most common *Elastic modulus.* It sometimes is called the modulus of elasticity, but this is more general since "bulk modulus" and "shear modulus" are in the modulus of elasticity category too. The values of elastic modulus derived from both real and engineering stress-strain graphs of Figure 4.11 are similar. Tensile modulus (Young's modulus) values obtained by tensile test are presented in Figure 4.12. Each column represents the average of Young's modulus calculated form 4 replicas. The results show an almost linear increasing trend up to 40 wt. % of bioglass filler, followed by a steeper increase with further increasing the added amounts of FastOs®BG Di–70. These observations are consistent with the a more than seven fold higher stiffness of the inorganic component (2770 MPa) as determined from compressive tests in the present work, relative to that of the PCL matrix (385 MPa), determined under tensile tests Figure 4.12.

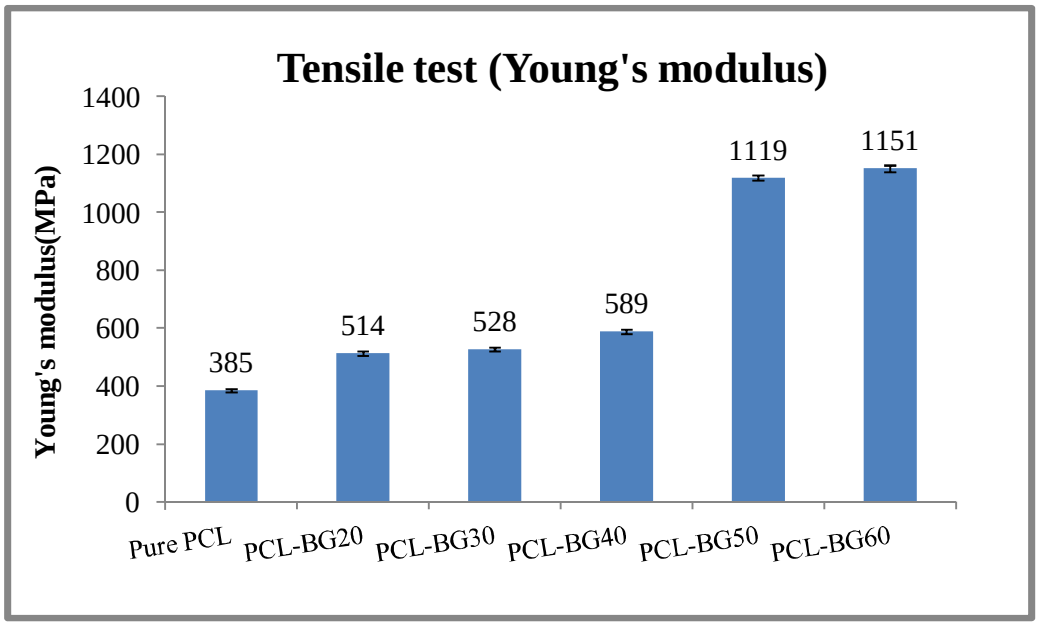

Figure 4.12: Young's modulus bar graph of all compositions

Several literature reports referred to in Table 4.2 revealed that the mechanical properties of PCL determined under tensile tests depend on a number of experimental parameters related to manufacturing methods of the testing samples, PCL molecular weight, strain rate, etc. The average value obtained in the present work is close to the higher values reported for injection moulded samples.

Table 4.2: Mechanical properties of bulk PCL in the literatures [57]

Reference	Manufacturing method	Tensile Modulus (MPa)	Tensile Strength (MPa)	Weight average Molecular weight, (Mn)	Number average molecular weight, (Mw)
Perstorp	Injection moulding	430	-	47500	84500
Pitt et al.	Melt extruding	264.8	-	50900	84500
Wehrenberg	Compression moulding	340	19.3	-	-
Feng et al.	Compression moulding	-	21.6	45000	50400
Engelberg	Compression moulding	400	16	42500	72500
Vandamme and Legras	Compression moulding	251.9	N/A	50500	101000
Rosa et al.	Compression moulding	429.1	16.9	50000	80000
Corello	Injection moulding	378	27.3	64000	124000
Granado	Injection moulding	300	14	-	80000

4.1.4. Applicability of the exiting theoretical models for predicting Young's modulus

Among the models presented in Table 2.2, only the applicability of the simplest ones will be tested in this work. The reasons behind are the isometric shape of the FastOs®BG Di–70 bioglass particles and the lack of information about the interfacial bonding strength between the two components. The ability of the Einstein's model to describe the experimental relative elastic modulus data derived from tensile strength measurements was tested. The relevant data reported in Table 4.3, was also plotted in Figure 4.13 for an easy visualisation. It can be seen that a reasonable agreement

could be obtained up to filler fractions of about 20 vol. %. This is not surprising considering that the applicability of this model is limited to small volume fractions of inorganic filler.

Table 4.3: Experimental values for Einstein's model

Composite Name	E_C / E_M (experimental)	V_p (%)	$E_C / E_M = 1+2.5\ V_P$ (calculated)
PCL-BG20	1.34	8.84	1.22
PCL-BG30	1.37	14.25	1.36
PCL-BG40	1.53	20.54	1.51
PCL-BG50	2.90	27.94	1.69
PCL-BG60	2.99	36.77	1.92

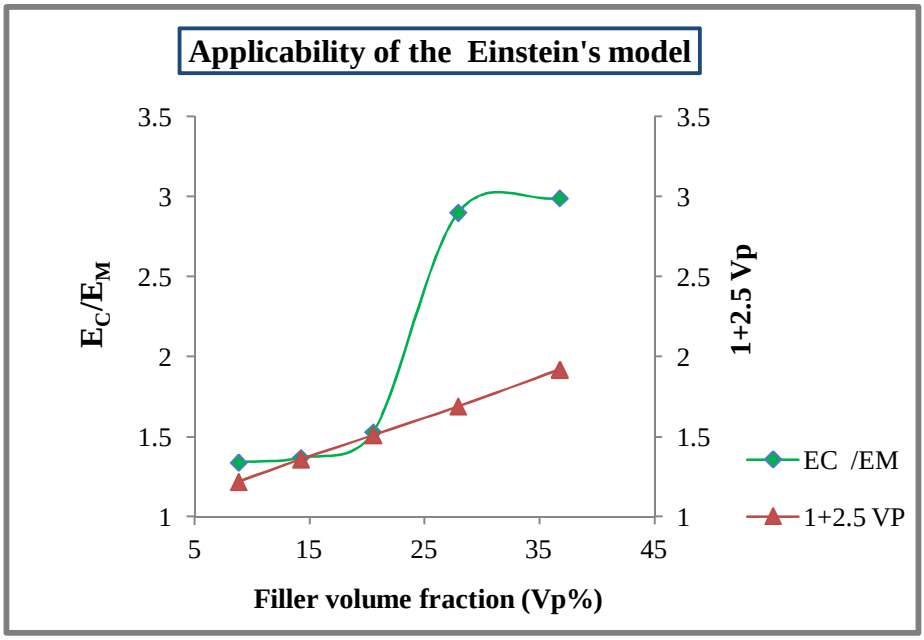

Figure 4.13: Comparison between experimental and predicted values by the Einstein's model

Young's modulus reflects the stiffness of a material at the elastic stage under tensile tests. The results obtained clearly prove that the addition of rigid particles to a polymeric matrix significantly decreased the ultimate strength in comparison to the neat polymer. The adhesion between organic and inorganic phases is a relevant parameter that determines the elastic modulus of a composite. A strong bonding between the polymer matrix and the reinforcing phase is a necessary condition for an effective load transfer and for improving the strength of a composite material. The effectiveness of load transfer is also strongly dependent on the aspect ratio of the reinforcing component. In the present case, the particles are isometric. On the other hand, from the different hydrophobic/hydrophilic nature of PCL and FastOs®BG Di–70 bioglass the bonding strength between both components is not expected to be strong.

To check the applicability of the rule of mixtures (lower bond and upper bond limits), the elastic modulus value of the FastOs®BG Di–70 bioglass determined under compressive tests (2770 MPa) was adopted together with the elastic modulus of PCL (385 MPa) obtained under tensile tests. The experimentally measured values and the calculated ones are reported in Table 4.4. They have also been plotted in Figure 4.14 for an easy visualisation. It can be seen that the experimental values up to filler fractions of about 20 vol.% lie in between the calculated ones using the lower and upper limits. For higher volume fractions the measured experimental values are superior to the maximum predicted ones. Further experiments will be necessary to better explain these unexpected results.

Table 4.4: Elastic modulus of composites calculated by the role of mixtures

Composite Name	**V_f (%)**	**E_C (experimental)**	**$E_C=E_fE_m/(E_fV_m+E_mV_f)$ (lower bond)**	**$E_C=E_fV_f+E_mV_m$ (upper bond)**
PCL-BG20	8.84	514	416.73	595.83
PCL-BG30	14.25	528	438.84	724.86
PCL-BG40	20.54	589	467.72	874.88
PCL-BG50	27.94	1119	506.95	1051.37
PCL-BG60	36.77	1151	563.36	1261.96

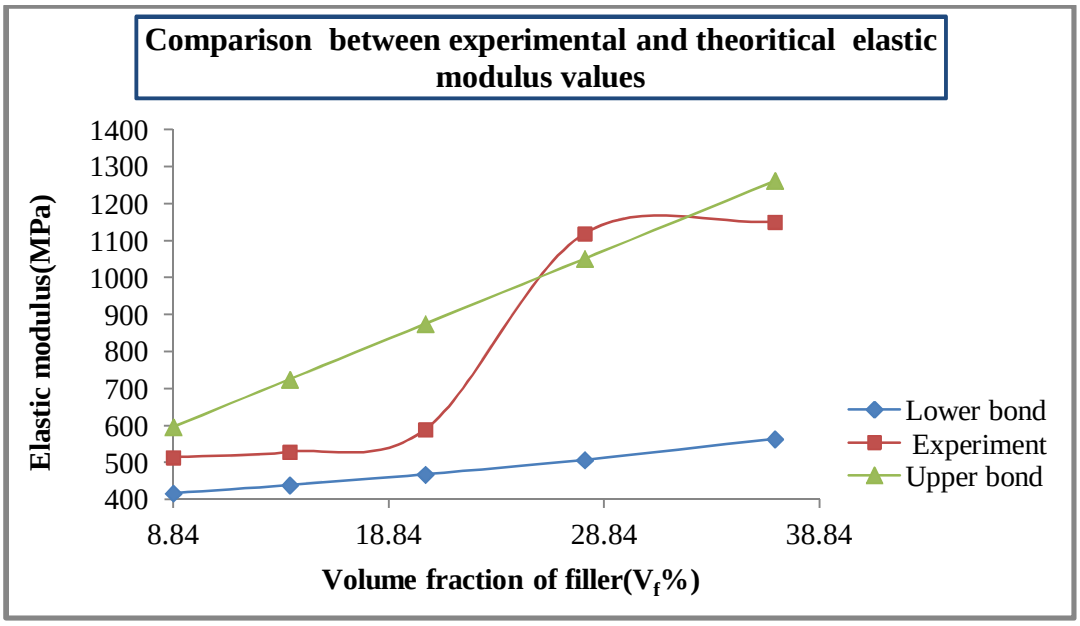

Figure 4.14: Experimental and predicted (by rule of mixtures) values of elastic modulus determined under tensile tests

4.2. Compressive test

The exact stress-strain characteristics of plastic materials are highly dependent on factors such as the rate of applied stress, temperature, previous history of specimen, etc. However, stress-strain curves for plastics, almost always show a linear region at low stresses, and a drawn straight line tangent to this portion of the curve permits the calculation of the elastic modulus.

The Young's modulus is defined as the slope of linear part of the curve.

$$\delta = E.\varepsilon \tag{4.6}$$

δ_N is the engineering stress, and defines as:

$$\delta_N = \frac{4P}{\pi D^2} \tag{4.7}$$

where **P** is the pressure and **D** is the sample diameter. ($\boldsymbol{\pi D^2}$) is the basal area of a cylindrical sample.

ε_N is engineering strain and it obtains by the ratio of the samples stroke (L) to the initial length of the sample (L_0).

$$\varepsilon_N = \frac{L}{L_0} \tag{4.8}$$

δ_R is real stress and it is obtained from the equation below:

$$\delta_R = (1+\varepsilon_N)\ \delta_N \tag{4.9}$$

where δ_R is real stress, ε_N is engineering strain and δ_N is engineering stress.

The real strain (ε_R) and the engineering strain (ε_N) are related through the following equation:

$$\varepsilon_R = LN\ (1+\varepsilon_N) \tag{4.10}$$

Unlike various published data about tensile mechanical properties of PCL, there are only limited data on the bulk compressive mechanical properties of PCL from literature reports. The compressive strength of bulk PCL was reported as 38.7 MPa, while the compressive modulus ranged from 297.8 to 317.1 MPa [57].

The mechanical properties of 3 selected compositions (pure PCL + 2 composite mixtures with the highest added amounts of bioactive glass) determined under tensile and compressive tests are compared in Table 4.5. Compressive modulus was obtained from the linear part of real stress-strain graphs (not shown).

Table 4.5: Comparison between strength of composites by tension and compression test

Composite code	Compressive modulus (MPa)	Compressive strength at ε=0.04 (MPa)	Tensile strength at ε=0.04 (MPa)
Pure PCL	319 ± 3.7	15.10	13.76
PCL-BG50	342 ± 2.4	17.53	10.75
PCL-BG60	353 ± 1.8	18.21	8.62

It can be seen that for an arbitrarily selected strain point (ε = 0.04), the elastic modulus increased with increasing amounts of bioactive glass. The same trend is observed for the compressive strength of the composites, in opposition to what happened for tensile strength. The increase in compressive strength can be understood considering that the composites become gradually stiffer as the fraction of inorganic component increases. On the other hand, the role of the interfacial bond between the matrix and the filler is less critical under this testing mode. The compressive pressure tends to compact the material and the flow tends to be hindered with increasing inorganic volume fractions. The contrary situation is expected when samples are tested under tensile mode. The continuity of matrix is disturbed by the incorporation of inorganic particles, which are relatively isometric, thus being not effective in sharing the applied tensile load because of a less efficient load transfer from the matrix to the filler in comparison to the effect promoted by high aspect ratio reinforcing agents. The load transfer is only due to the interfacial bond strength, which is not expected to be high considering the relatively hydrophobic nature of the PCL and the more hydrophilic character of the bioactive glass particles. Moreover, the deformation of the samples under tensile load is likely leading to the formation of voids and hollow spaces that turn the samples gradually less mechanical resistant.

Therefore, from the results presented and discussed above, it can be concluded that under compressive testing mode the addition of rigid bioactive particles increased the mechanical properties (compressive modulus and strength) of composites, while the tensile strength decreased as shown in Table 4.5. The different evolutions of compressive strength and tensile strength as a function of filler volume fraction can be understood considering that the formation of voids in the testing specimen is not expected under compressive mode, oppositely to what happens under tensile mode. However, the observed differences in values of elastic modulus determined by both testing modes seem more difficult to fully explain. One possible reason is the fact that compressive and tensile tests were

performed in different mechanical testing machines and under different strain rates (according to the specific standards). On the other hand, elastic modulus determination being operator dependent is also likely to be affected by the selection of the data range for calculation, although the operator was the same here. The most probable cause of the significant differences measured for elastic modulus under compressive and tensile testing modes is likely to be related to the different strain rates used and also to the typical shapes of the stress-strain curves obtained under the different testing modes. At the beginning of the test the slop is steeper under tensile tests, while there was a transient region at the initial portion of the curve before entering in the apparent Newtonian regime where elastic modulus can be derived from.

4.3. DMA test

Dynamic Mechanical Analyser (DMA) was used in the present work to study the frequency dependence of storage and loss modulus of composites with various filler volume proportions by applying an oscillatory (sinusoidal) force to the material at a constant temperature 37ºC (body temperature).

The applied frequency range defined for most of instruments is 0.01 to 100 Hz. Although it is more reasonable using a range which material will be expose to in real applications, it might be difficult in certain cases to define the accurate limits. Table 4.6 shows the applied frequencies used for testing some materials [25][58]. Excessively high frequencies are likely to harm the molecular structure of polymers and polymer matrix composites. Also considering the eventual application of our composite materials for fixation screws and a hand screwing operation, a frequency range of 0.01 to 1 Hz was selected to study the mechanical behaviour of the composites under oscillatory testing mode.

The complex modulus is a measure of the materials resistance to deformation [56][59]. It encompasses both in-phase and out-of phase response of the sample, from which one calculates the storage modulus E′ and the loss modulus E″ respectively:

$$E^*(\omega) = E'(\omega) + iE''(\omega) \qquad (4.11)$$

Table 4.6: Standard frequency range for some biomaterials

Common products and their use frequencies	
Paint levelling	0.01 Hz
Heart valves	1.2 Hz
Latex gloves and condoms	2 Hz
Plastic hip joints	4 Hz
Chewing, dental fillings	10 Hz
Contact lenses	16 Hz
Airbag openings	10000 Hz

Complex modulus covers both elastic and viscous components of the material. It can be determined directly by the Machine's software. The elastic modulus, or storage modulus E′ is a measure of the elastic energy stored and the viscous modulus, or loss modulus E″ is a measure of the energy lost [25][56][59][60]. To better understanding the concept of these two parameters, when a ball is bounced, the recovered energy describes as E′ and the difference between the height dropped from and the bounce called E" Figure 4.15.

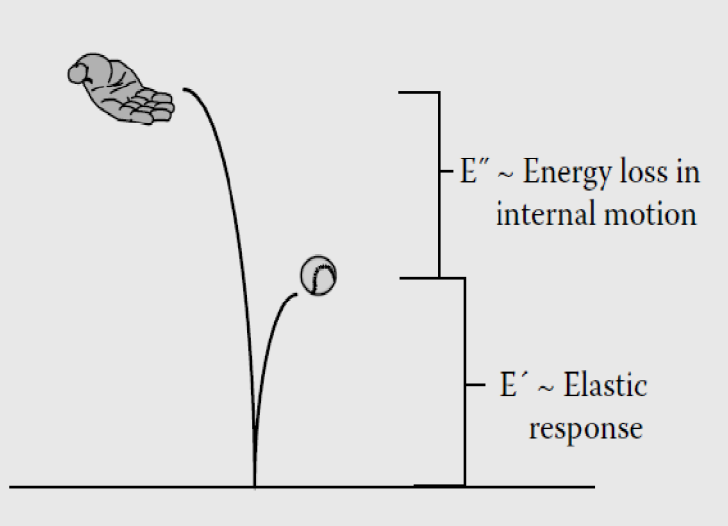

Figure 4.15: Schematic representation of the elastic modulus and loss modulus [56]

The storage modulus is defined as: $$E' = \frac{\delta_0}{\varepsilon_0} cos\delta \quad (4.12)$$

While loss modulus is given by: $$E'' = \frac{\delta_0}{\varepsilon_0} Sin\delta \quad (4.13)$$

The evolution of the complex modulus of different composites within the frequency range from 0.1 to 1 Hz is shown in Figure 4.16. Each line is the mean of 5 replicates. It can be seen that increasing the proportion of the filler in the composites increased the complex modulus. Also for all composites the complex modulus increased gradually from 0.1 to 1 Hz. In the case of pure PCL, complex modulus is almost constant along the entire frequency range. Behaviours close to this one are also observed for composites with the lower added amounts of filler up to 30 wt. %. The general overview of the complex modulus graphs clearly reveals that incrementing particle loading could significantly enhance the composite resistance to deformation. The increasing slope of the straight lines for higher filler fractions (Figure 4.16) is consistent with the enhanced stiffness of composite materials as explained above for results obtained under other testing modes.

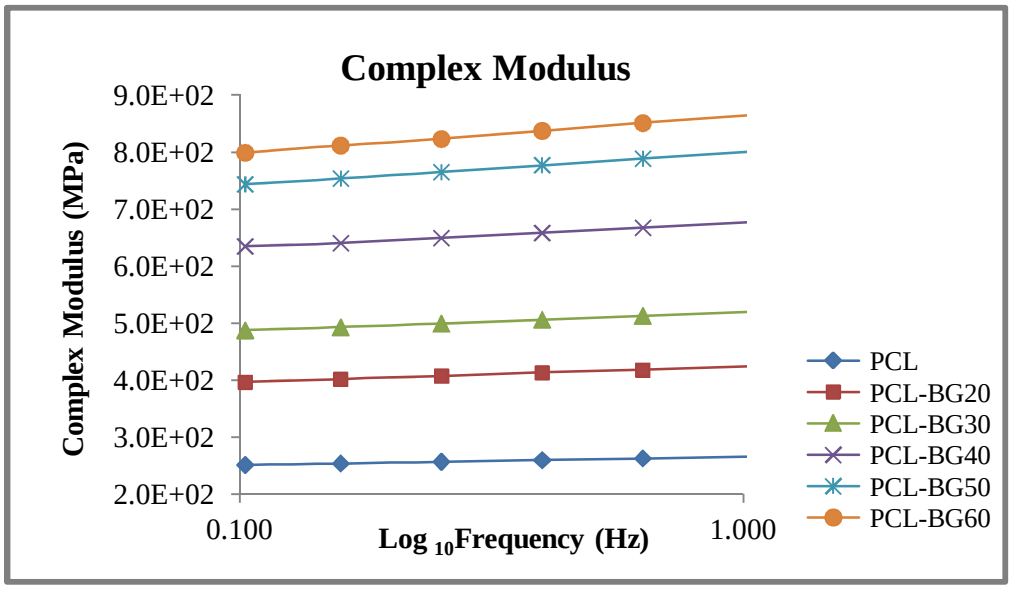

Figure 4.16: Comparison between complex modulus of all composites

The plots of storage modulus (E') and loss modulus (E") against log frequency are presented in Figure 4.17, and Figure 4.18, respectively. It can be seen that the plotted lines in Figure 4.17 look very similar to those shown in Figure 4.16 for complex modulus. From Pure PCL up to 30 wt.% (14.25 vol.%) filler the elastic modulus is almost independent of the frequency within the range tested. The incorporated amount of bioactive glass filler is the main factor determining the storage modulus (E'), which varies within the range from 254 – 265 MPa (pure PCL), and within the range from 808 – 861 MPa (PCL-BG60). These values are in relatively good agreement with those determined from tensile tests, expecting for the composites with higher fractions of filler. This is not surprising considering that the same shaping method (injection moulding) was used for preparing the testing specimens for tensile and DMA testing. It can also be concluded that compressive testing seems to be less prone to assess the elastic properties of the composite materials.

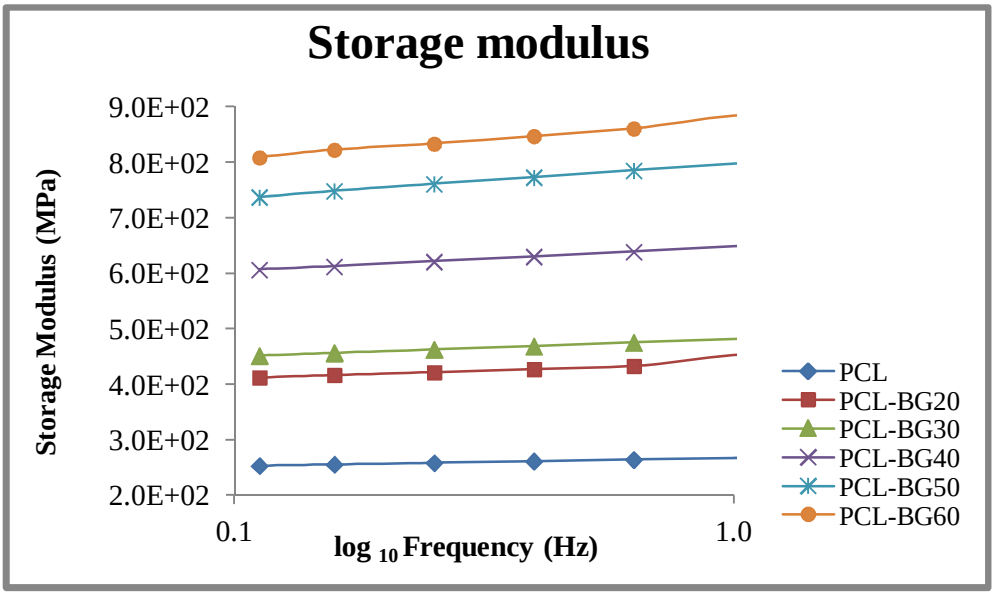

Figure 4.17: Comparison between storage modulus of all composites

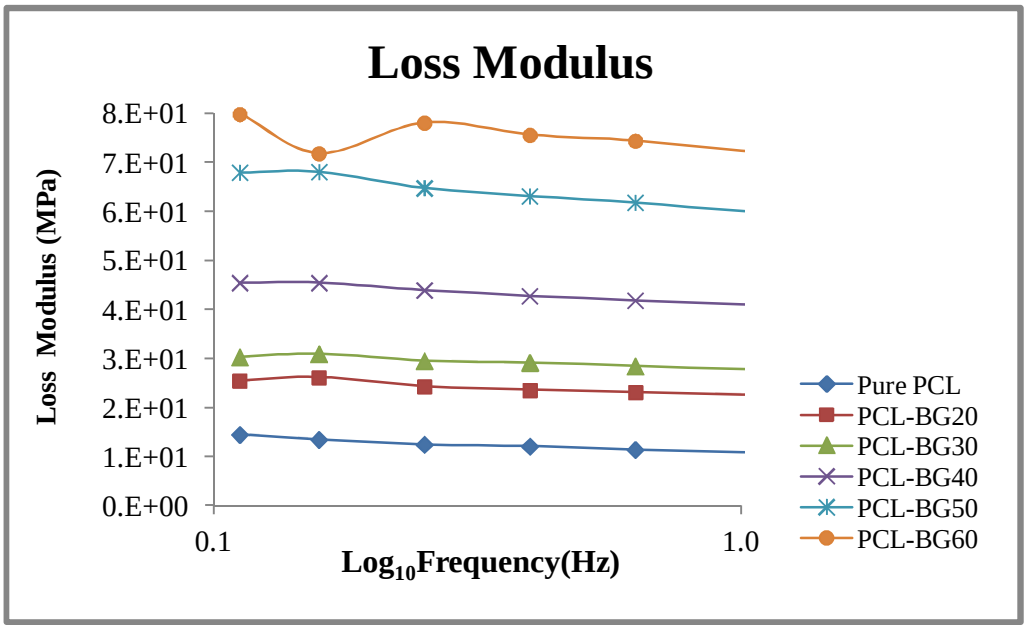

Figure 4.18: Loss modulus versus frequency comparison for all composites

The increasing trend of storage modulus with frequency is related to the shorter time allowed for the molecules to relax. Therefore, the composite system becomes stiffer and stiffer. In contrast to E', the plotted loss modulus (E") values against log frequency shows a decreasing trend. This variation is in good consistency with the observed evolution of the elastic modulus and their schematic representations in Figure 4.15. The loss modulus accounting for the lost energy in internal motion gives an idea about changes in the state of molecular motion. Since the storage modulus and loss modulus are complementary values for a given system, the increasing of the elastic proportion of the complex modulus will result in a decrease of the loss modulus as observed.

4.3.1. Reinforcing efficacy of the filler

The properties of polymeric composites depend primarily on the relative amounts and properties of the filler and matrix as well as the quality of interaction or interface between them. The shape of the particles and efficiency of dispersion and packing of the filler also influence the

magnitude of the enhancement [25]. To analyse the efficacy of the filler, relative modulus (E_r^I) values could be calculated according to Equation:

$$E_r^I = \frac{E_c^I}{E_m^I} \tag{4.14}$$

where E_c^I and E_m^I are the storage moduli of the composite and matrix, respectively, at a specific temperature. Table 4.7 presents the efficacy of filler calculated for all the composites. Final results show that higher filler volume fraction in the composite enhance the efficacy of the filler.

Table 4.7: Calculated efficiency of filler in various composites

Composite	Reinforcing efficiency of filler
Pure PCL	–
PCL-BG20	1.641
PCL-BG30	1.790
PCL-BG40	2.404
PCL-BG50	2.945
PCL-BG60	3.236

4.3.2. Loss factor

Loss factor (Tan δ) indicates the mechanical damping or internal friction in a viscoelastic system. It shows how well a material could get rid of the energy. In composite materials, weak interfacial bonding will dissipate more energy in comparison to the condition involving a strong bond between the components. So better interfacial bonding between matrix and filler in a composite system will result lower loss factor. In the present case, the magnitude of the interfacial bonding is not expected to change with varying filler volume faction. However, the continuity of the PCL matrix is disturbed more and more with increasing the added proportions of bioactive glass particles. In practice, this could be regarded a continuous decrease of the intrinsic bonding among PLC molecules, therefore, having an effect similar to that expected from a decreasing of the interfacial bonding. The measured damping (loss factor) data for all the compositions at the lowest and highest frequencies presented in Table 4.8 are according to this interpretation.

Table 4.8: Loss factor for various composites in 0.1 to 1Hz range

Composite code	Tan δ (at 0.1 HZ)	Tan δ (at 1 HZ)
Pure PCL	5.72E-02	4.33E-02
PCL-BG20	6.19E-02	5.35E-02
PCL-BG30	6.71E-02	5.99E-02
PCL-BG40	7.50E-02	6.55E-02
PCL-BG50	9.21E-02	7.87E-02
PCL-BG60	9.88E-02	8.63E-02

In particulate composites, the energy loss mechanism (damping) induced by the polymer matrix is complex. There is the possibility of additional loss mechanisms occurring at the filler–matrix interface, which are dependent on the extent of adhesion between the phases [25]. The filler contribution to damping is extremely low compared to the matrix. Considering that damping is only dependent on the volume fraction of the matrix, the Equation is:

$$V_m = \frac{\tan \delta c}{\tan \delta m} \quad (4.15)$$

or

$$V_m = \frac{E''_c \times E'_m}{E'_c \times E''_m} \quad (4.16)$$

where V_m is the volume fraction of the matrix in a composite, tan δ_c is the damping of the composite, and tan δ_m is the damping of the unfilled polymer. On the other hand, in the Equation 4.16, $\frac{E'_m}{E''_m}$ is constant as it refers to the pure PCL matrix.

If the damping in a filled polymer results from the same mechanism as produces the damping in the unfilled matrix then the ratio expressed by equation 4.16 holds. However, it is possible that new damping mechanisms may be introduced that are not present in the unfilled polymer, which include

particle–particle friction where particles are in contact with each other in the weak agglomerates that occur at high volume fractions [25].

Table 4.9: Comparison between volume fraction of matrix in the composite and loss tangent ratio given by equation 4.16 at two different frequencies

Composite code	$\mathbf{V_m}$ (matrix volume fraction)	$\boldsymbol{Tan\,\delta_c/Tan\,\delta_m}$ **(**at 0.1Hz**)**	$\boldsymbol{Tan\,\delta_c/Tan\,\delta_m}$ **(**at 1.0 Hz**)**
Pure PCL	1.0	–	–
PCL-BG20	0.9116	1.08	1.23
PCL-BG30	0.8575	1.17	1.38
PCL-BG40	0.7946	1.31	1.51
PCL-BG50	0.7206	1.60	1.82
PCL-BG60	0.6323	1.73	1.99

4.4. Torsional tests

There are different factors which can effect on the final results of torsion test. The applied torque, speed rate of rotation, clamping type and geometry of the specimens all can have influence on the final results. In the present work, both temperature and the type of clamping were always the same for all tests. A maximum torque of 40 N.m was also applied to all samples at a rate of 50 mm min^{-1}, as described in Chapter 3.

The exported results from the machine and video extensometer were presented in a predefined macro in excel software, which renders angle of twist (θ) versus applied torque (*T*). The graphical relationship of the torque *versus* degree of rotation is plotted in Figure 4.19a. Slope of the linear portion of graph, which demonstrates elastic behaviour of the samples, is shown in Figure 4.19b.

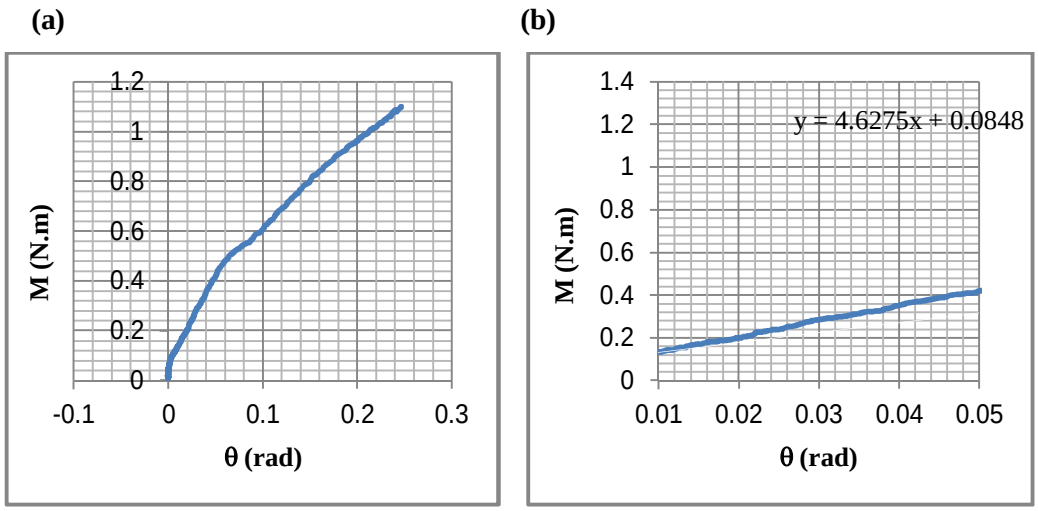

Figure 4.19: Torque *versus* rotaion angle **(a);** Initial linear part of diagram "**a**" corresponding to the elastic behaviour **(b)**.

4.4.1. Calculations

For a bar of uniform cross-section along its length:

$$\theta = \frac{TL}{JG} \tag{4.17}$$

Where

θ is the angle of twist in radians

T is the applied torque

L is the bar length

J is the second Polar Moment of Area

G is the Modulus of rigidity (shear modulus) of the material

For rectangle bars:

$$J = \beta a b^3 \tag{4.18}$$

Where

a is the length of the long side

b is the length of the short side

β is found from the Table 4.10:

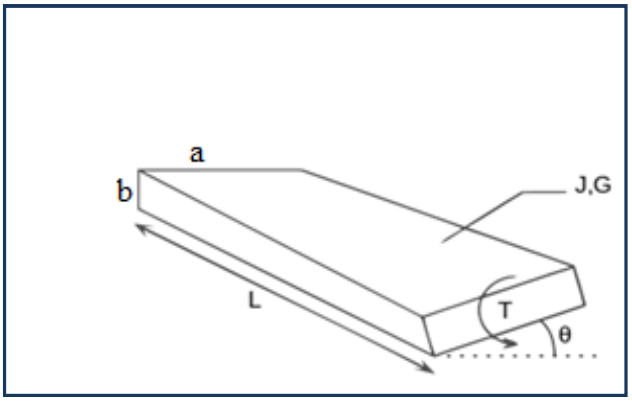

Figure 4.20: Schematic bar shape and sample dimensions

Table 4.10: Width to thickness ratio and constant value for each proportion (β)

a/b	1.0	1.5	2.0	2.5	3.0	4.0	5.0	6.0	10	∞
β	0.141	0.196	0.229	0.249	0.263	0.281	0.291	0.299	0.312	0.333

$$\text{Slope} = \frac{T}{\theta} \tag{4.19}$$

For a uniform cross-section sample along its length:

$$G = \frac{TL}{J\theta} \longrightarrow G = \frac{T}{\theta} \times \frac{L}{J} \longrightarrow G = \text{Slope} \times \frac{L}{J} \tag{4.20}$$

All the calculations are presented in Table 4.11. In ideal condition the geometry of the samples is exactly the same, so there will be a proportional relationship between $\frac{T}{\theta}$ and G modulus. But since in the present work there are small differences between the sizes of samples, this factor also has to be considered in calculations. The average shear modulus values for each selected composites are displayed in Figure 4.21.

Table 4.11: Modulus of rigidity calculation steps for three different composites

Code / Parameter	Pure PCL			PCL-BG20			PCL-BG50		
	Sample			Sample			Sample		
	1	2	3	1	2	3	1	2	3
a *(mm)*	8.62	8.60	8.63	8.63	8.61	8.62	8.59	8.61	8.60
b*(mm)*	8.50	8.51	8.50	8.50	8.51	8.50	8.51	8.50	8.51
$\beta = \frac{a}{b}$	0.141	0.141	0.141	0.141	0.141	0.141	0.141	0.141	0.141
$J = \beta a b^3$	746.42	747.32	747.28	747.28	748.18	746.41	746.45	745.55	747.32
$\frac{T}{\theta}$ (Slope)	3.24	3.37	3.32	4.00	4.11	4.13	4.63	4.81	4.69
$G = \frac{Slope}{J} * L$ (MPa)	95	99	97	117	120	122	136	142	138

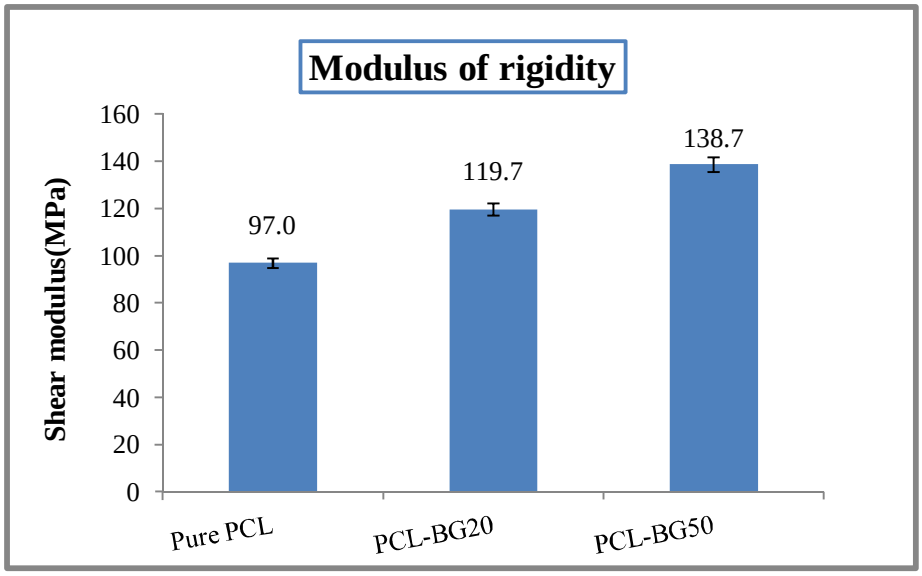

Figure 4.21: Shear modulus values of different composites

Shape of the filler, filler volume fraction and adhesion between phases are parameters that affect the shear modulus of filled composites. In the present study, only the filler fraction was changed. So, differences between shear modulus of the composites will result mostly from this variable.

One of the earliest theories for composite systems made of rigid inclusions in non-rigid matrix was based on Einstein's equation. Early this equation defined based on the viscosity of a suspension of rigid spherical inclusions as:

$$\eta_c = \eta_m(1 + K_E V_p) \tag{4.21}$$

Where η_c and η_m are the viscosity of suspension and the matrix, respectively. K_E is the Einstein coefficient which is equal to 2.5, for spheres. V_p is the volume fraction of particulate inclusions [13][37][45].

It has been demonstrated that there is a simple relationship between relative viscosities and relative shear moduli [60]:

$$\frac{\eta_c}{\eta_m} = \frac{G_c}{G_m} \tag{4.22}$$

So that Equation 4.21 for shear modulus can be written as:

$$G_c = G_m(1 + 2.5\ V_p) \tag{4.23}$$

where G is the shear modulus and p, m and c refer to particle, matrix and composite, respectively.

Einstein equation implies that stiffening action of filler is depending on volume occupied by the filler, not its weight. Experimental results are consistent with Einstein's theory only for low concentration of filler. Results shows that in the case of PCL-BG50 composite which contains approximately 28 vol.% filler, Einstein's equation does not matched the experimental results. By increasing the volume fraction of filler, the flow or strain fields around particles interact and Einstein equation is not able to explain these interactions.

Kerner equation is another theoretical way to calculate the modulus of rigid-particulate filled polymeric composites [9].

$$G_C = G_m\left(1 + \frac{V_p}{V_m}\frac{15(1-\nu_m)}{(8-10\nu_m)}\right) \tag{4.24}$$

In equation 4.24, ν_m is Poisson ratio of the matrix, which is obtain by negative of the initial slope of the transverse strain-longitudinal strain curve in tensile test. Poisson ratio of the pure PCL (polymeric matrix) was calculated around 0.48.

Poisson ratio value of pure PCL obtained from the experimental result is very close to the theoretical determined results

In general addition of rigid particles in to a polymer matrix can easily improve the stiffness and Young's modulus. Since the rigidity of inorganic fillers is generally much higher than that of organic polymer, the composite modulus consistently increases by increasing particle loading in the composite. As an overview it is assumed that changes in relative filler content will be parallel with the increase in shear modulus.

CHAPTER 5

5. CONCLUSIONS AND FUTURE WORK

Polycaplolactone matrix reinforced with FastOs®BG Di−70 bioglass weight fractions up 60% were successfully prepared by hot pressing and injection moulding and their mechanical properties were assessed through different testing modes. The results obtained showed that composite mechanical properties are closely related to the proportion of incorporated bioactive glass filler. As general trends, the presence of filler particles enhanced some properties like density and stiffness of composites, while caused opposite variations on their ultimate tensile strength. Moreover, the following specific main conclusions can be drawn from the results presented and discussed along this thesis:

1. Tensile strength results clearly showed that the gradual addition of rigid particles to the polymer matrix led to a concomitant decreased the ultimate strength in comparison to the neat polymer. For example, the real tensile strength measured for PCL-BG60 was about one half of that of pure PCL. This decreasing trend is attributed to an inefficient load transfer from the matrix to the isometric inclusions and to a poor interfacial bonding between the two components. This last feature was expected considering the relatively hydrophobicity nature of the polymer that contrasts with the hydrophilic character of bioglass filler particles.

2. Compressive test results showed that the gradual incorporation of rigid bioactive glass particles increased the compressive strength and modulus of composites. Such opposite behaviour relatively to tensile testing can be understood considering that the transfer load mechanism under compression is much less dependent to the interfacial bonding strength between the two components. In this case, instead of voids creation in the testing specimen, any pre-existing voids will tend to be filled. These features made compressive testing less suitable for predicting the mechanical behaviour/properties of the composites than tensile testing.

3. DMA testing revealed to be very appropriate to assess the viscoelastic properties of the composites. The E' was found to increase with the addition of filler volume fractions. In general it was observed that composites with higher proportions of bioglass had higher storage modulus in comparison to pure polymer. The materials behaviour within the tested frequency range was almost constant at lower proportions of filler and tended to become gradually more accentuated with increasing filler volume fractions. Obtained results for loss factor and filler efficiency also support this idea that composites with higher volume fractions of rigid filler are stiffer.

4. Torsion test results also showed the addition of rigid particles in to the PCL matrix caused a general improvement of the stiffness and Young's modulus of composite materials, in close agreement with the higher rigidity of inorganic filler particles. The shear modulus roughly scaled with the relative filler contents in the composites.

Further work

Due to time limitations, it was not possible to explore all the relevant aspects related to the topic, which might influence the performance of the composites upon use when considering their intended functional applications, including the *in vitro* bioactivity and degradation rates. Also, the mechanical properties are likely to be enhanced by increasing the interfacial bonding strength between the components. This could probably be achieved by using coupling agents. Another factor which is worthy to investigate is the used of effect of a PCL matrix with higher molecular weight, as literature reports suggest that polymers with higher molecular weights show higher strength in compare to lower molecular weight polymers. Therefore, these aspects stand as a future research lines.

6. References

[1] J.C. Middleton and A.J. Tipton, "Synthetic biodegradable polymers as orthopedic devices.," *Biomaterials*, vol. 21, no. 23, pp. 2335–46, Dec. 2000.

[2] J. E. Bergsma, W. C. de Bruijn, F. R. Rozema, R. R. Bos, and G. Boering, "Late degradation tissue response to poly(L-lactide) bone plates and screws.," *Biomaterials*, vol. 16, no. 1, pp. 25–31, Jan. 1995.

[3] M. A. Woodruff and D. W. Hutmacher, "The return of a forgotten polymer—Polycaprolactone in the 21st century," *Prog. Polym. Sci.*, vol. 35, no. 10, pp. 1217–1256, Oct. 2010.

[4] L. S. Nair and C. T. Laurencin, "Biodegradable polymers as biomaterials," *Prog. Polym. Sci.*, vol. 32, no. 8–9, pp. 762–798, Aug. 2007.

[5] Marta Hrabalova. PhD Thesis (2011). *Viscoelastic and thermal properties of natural fiber-reinforced composites*. University of Natural Resources and Life Sciences Vienna.

[6] Elgozali A. and Hassan M., "EFFECT OF ADDITIVES ON THE MECHANICAL PROPERTIES OF POLYVINYL CHLORIDE," *J.Sc. Tech*, vol. 9, no. 1, pp. 1–12, 2008.

[7] R. S. Lakes, *Viscoelastic Materials Hand book*. Cambridge University Press, 2009, Chapter 9, pp. 341–345.

[8] Patel, R.; Gohil, P. "A Review on Biomaterials: Scope, Applications & Human Anatomy Significance," *Int. J. Emerg. Technol. Adv. Eng.*, vol. 2, no. 4, pp. 91–101.

[9] Ahmad, S. ,F.R. Jones, "A review of particulate reinforcement theories for polymer composites," *Mater. Sci.*, vol. 25, pp. 4933–4942, 1990.

[10] A. Goel, S. Kapoor, R. R. Rajagopal, M. J. Pascual, H.-W. Kim, and J. M. F. Ferreira, "Alkali-free bioactive glasses for bone tissue engineering: a preliminary investigation.," *Acta Biomater.*, vol. 8, no. 1, pp. 361–72, Jan. 2012.

[11] A. R. Chen, Q., Roether, J.A. and Boccaccini, "Tissue Engineering Scaffolds from Bioactive Glass and Composite Materials," vol. 4, 2008.

[12] M. Kinsella, D. Murray, D. Crane, J. Mancinelli, and M. Kranjc, "MECHANICAL PROPERTIES OF POLYMERIC COMPOSITES REINFORCED WITH HIGH STRENGTH GLASS FIBERS." In *International SAMPE Technical Conference*, vol. 33, pp. 1644-1657. 2001.

[13] S.-Y. Fu, X.-Q. Feng, B. Lauke, and Y.-W. Mai, "Effects of particle size, particle/matrix interface adhesion and particle loading on mechanical properties of particulate–polymer composites," *Compos. Part B Eng.*, vol. 39, no. 6, pp. 933–961, Sep. 2008.

[14] S. Weiner and H. D. Wagner, "THE MATERIAL BONE: Structure-Mechanical Function Relations," *Annu. Rev. Mater. Sci.*, vol. 28, no. 1, pp. 271–298, Aug. 1998.

[15] M.P. Ginebra; J.A. Planell; M. Ontanon; C . Aparicio, "*Structural Biological Materials: Design and Structure-Property Relationships*". Elsevier, 2000, pp. 33–71

[16] S. C. Cowin, "Bone poroelasticity," *J. Biomech.*, vol. 32, no. 3, pp. 217–238, Mar. 1999.

[17] S. C. Miller and W. S. S. Jee, "The bone lining cell: A distinct phenotype?," *Calcif. Tissue Int.*, vol. 41, no. 1, pp. 1–5, Jan. 1987.

[18] A. Sarmiento, P. Kinman, and E. Galvin, "Functional bracing of fractures of the shaft of the humerus," *J Bone Jt. Surg* …, 1977.

[19] A. Sarmiento, "Functional bracing of tibial fracture," *Clin Orthop Rel Res*, vol. 105, pp. 202–219, 1974.

[20] D. R. Carter and G. S. Beaupré, "Skeletal Function and Form: Mechanobiology of Skeletal Development, Aging, and Regeneration," p. 332, 2001.

[21] J. Black, *Biological Performance of Materials: Fundamentals of Biocompatibility, Fourth Edition*. New York, 1992.

[22] S. Ramakrishna, J. Mayer, E. Wintermantel, and K. W. Leong, "Biomedical applications of polymer-composite materials: a review," *Compos. Sci. Technol.*, vol. 61, no. 9, pp. 1189–1224, Jul. 2001.

[23] D. Pietrzak,S. ; Sarver, "Bioresorbable implants-practical consideration," vol. 19, no. 1, pp. 109–119, 1996.

[24] W. Cao and L. L. Hench, "Bioactive materials," *Ceram. Int.*, vol. 22, no. 6, pp. 493–507, 1996.

[25] P. Gabbott, *Principles and Applications of Thermal Analysis*. Blackwell, 2008, pp. 261–264.

[26] W. Hench, Larry L., Cao, "Bioactive Materials," *Ceram. Int.*, vol. 8842, no. 95, pp. 493–507, 1996.

[27] L. L. Hench, "The story of Bioglass.," *J. Mater. Sci. Mater. Med.*, vol. 17, no. 11, pp. 967–78, Nov. 2006.

[28] L. L. Hench and J. R. Jones, "Bioactive Materials for Tissue Engineering Scaffolds," pp. 3–24.

[29] G. W. Teoh, S.H.; Tang, Z.G.; Hastings, *Thermoplastic Polymers In Biomedical Applications: Structures, Properties and Processing*. London: Springer US, 1998, pp. 270–301.

[30] L. Eschbach, "Nonresorbable polymers in bone surgery.," *Injury*, vol. 31 Suppl 4, pp. 22–7, Dec. 2000.

[31] S. Gogolewski, "Bioresorbable polymers in trauma and bone surgery," *Injury*, vol. 31, pp. D28–D32, Dec. 2000.

[32] J. O. Hollinger, "Biomedical applications of synthetic biodegradable polymers," 1995. [Online]. Available: http://www.ecmjournal.org/journal/papers/vol005/pdf/v005a01.pdf. [Accessed: 04-Apr-2014].

[33] R. L. Wise, D.L.; Fellmann, T.D.; Sanderson, J.E.; Wentworth, *Lactic/glycolic acid polymers. In: Gregoriadis G, ed. Drug Carriers in Biology and Medicine*. London, 1979, pp. 237–270.

[34] I. Vroman and L. Tighzert, "Biodegradable Polymers," *Materials (Basel).*, vol. 2, no. 2, pp. 307–344, Apr. 2009.

[35] K. J. Lowry, K. R. Hamson, L. Bear, Y. B. Peng, R. Calaluce, M. L. Evans, J. O. Anglen, and W. C. Allen, "Polycaprolactone/glass bioabsorbable implant in a rabbit humerus fracture model.," *J. Biomed. Mater. Res.*, vol. 36, no. 4, pp. 536–41, Sep. 1997.

[36] R. Gunatillake, P.;Adhikari, "Biodegradable synthetic polymers for tissue engineering.," *Eur. Cell. Mater.*, vol. 5, pp. 1–16; discussion 16, May 2003.

[37] M. Bergstrom,s.,Boyce, "MECHANICAL BEHAVIOR OF PARTICLE FILLED ElASTOMERS," *Rubber Chem. Technol.*,, vol. 72, no. i, pp. 1633–656, 1999.

[38] F. L. Matthews and R. D. Rawlings, *Composite Materials: Engineering and Science*. CRC Press, 1999, p. 480.

[39] M. E. J. Dekkers and D. Heikens, "The effect of interfacial adhesion on the tensile behavior of polystyrene–glass-bead composites," *J. Appl. Polym. Sci.*, vol. 28, no. 12, pp. 3809–3815, Dec. 1983.

[40] D. S. Suprapakorn N, "Effect of CaCO3 on the mechanical and rheological properties of a ring-opening phenolic resin: polybenzoxazine.," *Polym Compos*, vol. 19, pp. 126–32, 1998.

[41] M. Wang, C. Berry, M. Braden, and W. Bonfield, "Young's and shear moduli of ceramic particle filled polyethylene.," *J. Mater. Sci. Mater. Med.*, vol. 9, no. 11, pp. 621–4, Nov. 1998.

[42] S. C. Tjong and S. A. Xu, "Ternary polymer composites: PA6,6/maleated SEBS/glass beads," *J. Appl. Polym. Sci.*, vol. 81, no. 13, pp. 3231–3237, Sep. 2001.

[43] G. J. Amdouni N, Sautereau H, "Epoxy composites based on glass-beats. 2. Mechanical-properties.," *Appl Polym Sci 1992*, vol. 46, pp. 1723–35, 1992.

[44] Y. Ou, F. Yang, and Z.-Z. Yu, "A new conception on the toughness of nylon 6/silica nanocomposite prepared viain situ polymerization," *J. Polym. Sci. Part B Polym. Phys.*, vol. 36, no. 5, pp. 789–795, Apr. 1998.

[45] W. Yan, R. J. T. Lin, and D. Bhattacharyya, "Particulate reinforced rotationally moulded polyethylene composites – Mixing methods and mechanical properties," *Compos. Sci. Technol.*, vol. 66, no. 13, pp. 2080–2088, Oct. 2006.

[46] Y. M. Wang, K. Wang, D. Pan, K. Lu, K. J. Hemker, and E. Ma, "Microsample tensile testing of nanocrystalline copper," *Scr. Mater.*, vol. 48, no. 12, pp. 1581–1586, Jun. 2003.

[47] S. Debnath, R. Ranade, S. L. Wunder, J. McCool, K. Boberick, and G. Baran, "Interface effects on mechanical properties of particle-reinforced composites.," *Dent. Mater.*, vol. 20, no. 7, pp. 677–86, Sep. 2004.

[48] V. P. Chacko, R. J. Farris, and F. E. Karasz, "Tensile properties of CaCO3-filled polyethylenes," *J. Appl. Polym. Sci.*, vol. 28, no. 9, pp. 2701–2713, Sep. 1983.

[49] A. Maazouz, H. Sautereau, and J. F. Gerard, "Hybrid-particulate composites based on an epoxy matrix, a reactive rubber, and glass beads: Morphology, viscoelastic, and mechanical properties," *J. Appl. Polym. Sci.*, vol. 50, no. 4, pp. 615–626, Oct. 1993.

[50] B. Pukanszky and G. VÖRÖS, "Mechanism of interfacial interactions in particulate filled composites," *Compos. Interfaces*, 1993.

[51] A. D. Drozdov and A. Dorfmann, "Finite Viscoelasticity of Particle-Reinforced Elastomers: the Effect of Filler Content," *Macromol. Theory Simulations*, vol. 11, no. 4, p. 383, Apr. 2002.

[52] G. F. London, G.; Lewis, G.; Booden, "The influence of particle size on the tensile strength of particulate-filled polymers," *J. Mater. Sci. 12*, vol. 12, pp. 1605–1613, 1977.

[53] "ASTM D638 - 10 Standard Test Method for Tensile Properties of Plastics." [Online]. Available: http://www.astm.org/Standards/D638.htm. [Accessed: 07-Mar-2014].

[54] I. Engelberg and J. Kohn, "Physico-mechanical properties of degradable polymers used in medical applications: A comparative study," *Biomaterials*, vol. 12, no. 3, pp. 292–304, Apr. 1991.

[55] "ASTM D695 - 10 Standard Test Method for Compressive Properties of Rigid Plastics." [Online]. Available: http://www.astm.org/Standards/D695.htm. [Accessed: 07-Mar-2014].

[56] H. Menard, *DYNAMIC MECHANICAL ANALYSIS*, Second. 2008, pp. 1–33.

[57] S. Eshraghi and S. Das, "Mechanical and microstructural properties of polycaprolactone scaffolds with one-dimensional, two-dimensional, and three-dimensional orthogonally oriented porous

architectures produced by selective laser sintering.," *Acta Biomater.*, vol. 6, no. 7, pp. 2467–76, Jul. 2010.

[58] J. H. Park and S. C. Jana, "The relationship between nano- and micro-structures and mechanical properties in PMMA–epoxy–nanoclay composites," *Polymer (Guildf).*, vol. 44, no. 7, pp. 2091–2100, Mar. 2003.

[59] D. M. Analysis, "Dynamic Mechanical Analysis (DMA) A Beginner ' s Guide Table of Contents."

[60] R. F. Landel and L. E. Nielsen, *Mechanical Properties of Polymers and Composites, Second Edition*. CRC Press, 1993, p. 580.

[61] R. M. Felfel, I. Ahmed, A. J. Parsons, and C. D. Rudd, "Bioresorbable composite screws manufactured via forging process : Pull-out , shear , flexural and degradation characteristics," *J. Mech. Behav. Biomed. Mater.*, vol. 18, pp. 108–122, 2013.